AD A0 65151

STUDY OF RADC NEWPORT ANTENNA TEST RANGE: METHODS OF REFLECTION REDUCTIONS AND INCREASED FREQUENCY COVERAGE

Syracuse University

DDC

ROME AIR DEVELOPMENT CENTER
Air Force Systems Command
Griffiss Air Force Base, New York 13441

This report has been reviewed by the RADC Information Office (OI) and is releasable to the National Technical Information Service (NTIS). At NTIS it will be releasable to the general public, including foreign nations.

RADC-TR-78-262 has been reviewed and is approved for publication.

APPROVED: *Jacob Scherer*

JACOB SCHERER
Project Engineer

APPROVED: *Joseph J. Naresky*

JOSEPH J. NARESKY
Chief, Reliability & Compatibility Division

FOR THE COMMANDER: *John P. Huss*

JOHN P. HUSS
Acting Chief, Plans Office

If your address has changed or if you wish to be removed from the RADC mailing list, or if the addressee is no longer employed by your organization, please notify RADC (RBC) Griffiss AFB NY 13441. This will assist us in maintaining a current mailing list.

Do not return this copy. Retain or destroy.

BEST AVAILABLE COPY

REPORT DOCUMENTATION PAGE		READ INSTRUCTIONS BEFORE COMPLETING FORM
1. REPORT NUMBER RADC-TR-78-262	2. GOVT ACCESSION NO.	3. RECIPIENT'S CATALOG NUMBER
4. TITLE (and Subtitle) STUDY OF RADC NEWPORT ANTENNA TEST RANGE: METHODS OF REFLECTION REDUCTIONS AND INCREASED FREQUENCY COVERAGE		5. TYPE OF REPORT & PERIOD COVERED Phase Report.
		6. PERFORMING ORG. REPORT NUMBER N/A
7. AUTHOR(s) J. Perini B. Silverman		8. CONTRACT OR GRANT NUMBER(s) F30602-75-C-0121
9. PERFORMING ORGANIZATION NAME AND ADDRESS Syracuse University Syracuse NY 13210		10. PROGRAM ELEMENT, PROJECT, TASK AREA & WORK UNIT NUMBERS 95670016 00
11. CONTROLLING OFFICE NAME AND ADDRESS Rome Air Development Center (RBC) Griffiss AFB NY 13441		12. REPORT DATE January 1979
		13. NUMBER OF PAGES 62 71 p.
14. MONITORING AGENCY NAME & ADDRESS(If different from Controlling Office) Same		15. SECURITY CLASS. (of this report) UNCLASSIFIED
		15a. DECLASSIFICATION/DOWNGRADING SCHEDULE N/A

16. DISTRIBUTION STATEMENT (of this Report)

Approved for public release; distribution unlimited.

17. DISTRIBUTION STATEMENT (of the abstract entered in Block 20, if different from Report)

Same

18. SUPPLEMENTARY NOTES

RADC Project Engineer: Jacob Scherer (RBC)

19. KEY WORDS (Continue on reverse side if necessary and identify by block number)

Antennas
Testing
Patterns

20. ABSTRACT (Continue on reverse side if necessary and identify by block number)

In this report a study of the short and long antenna ranges at the RADC/NEWPORT site is undertaken with the objectives of extending its frequency of operation from 2 GHz down to 200 MHz and from 18 GHz up to 40 GHz. In the report the problem of ground reflections is studied and two solutions are proposed. A short term solution was that of constructing ground fences and a long term solution which consists of processing the signal received using digital signal processing techniques to eliminate the reflections. The ground fences have been constructed and the improvement is documented by measurements before and

DD FORM 1473 EDITION OF 1 NOV 65 IS OBSOLETE
1 JAN 73

339 600

after the fences were installed. As for the digital signal processing a theoretical study is carried out. A feasibility study of its implementation is recommended. Instrumentation needs for the extension of the site frequency range is also included in the report.

PREFACE

This effort was conducted by Syracuse University under the sponsorship of the Rome Air Development Center Post-Doctoral Program for Rome Air Development Center. Mr. Charles Pankiewicz, RADC/RBTV, was the task project engineer and provided overall technical direction and guidance.

The RADC Post-Doctoral Program is a cooperative venture between RADC and some sixty-five universities eligible to participate in the program. Syracuse University (Department of Electrical Engineering), Purdue University (School of Electrical Engineering), Georgia Institute of Technology (School of Electrical Engineering), and State University of New York at Buffalo (Department of Electrical Engineering) act as prime contractor schools with other schools participating via sub-contracts with prime schools. The U.S. Air Force Academy (Department of Electrical Engineering), Air Force Institute of Technology (Department of Electrical Engineering), and the Naval Post Graduate School (Department of Electrical Engineering) also participate in the program.

The Post-Doctoral Program provides an opportunity for faculty at participating universities to spend up to one year full time on exploratory development and problem-solving efforts with the post-doctorals splitting their time between the customer location and their educational institutions. The program is totally customer-funded with current projects being undertaken for Rome Air Development Center (RADC), Space and Missile Systems Organization (SAMSO), Aeronautical System Division (ASD),

1

Electronics Systems Division (ESD), Air Force Avionics Laboratory (AFAL), Foreign Technology Division (FTD), Air Force Weapons Laboratory (AFWL), Armament Development and Test Center (ADTC), Air Force Communications Service (AFCS), Aerospace Defense Command (ADC), HQ USAF, Defense Communications Agency (DCA), Navy, Army, Aerospace Medical Division (AMD), and Federal Aviation Administration (FAA).

Further information about the RADC Post-Doctoral Program can be obtained from Mr. Jacob Scherer, RADC/RBC, Griffiss AFB, NY, 13441, telephone Autovon 587-2543, Commercial (315) 330-2543.

TABLE OF CONTENTS

LIST OF ILLUSTRATIONS

1. INTRODUCTION

1.1 Background

The Newport Antenna Test Range of Rome Air Development Center is concerned with the testing and evaluation of ground-based and aircraft-mounted antennas.

At present, its principal test sites are located on Tanner Hill and Irish Hill as indicated in Figure 1.

A number of studies have been conducted in the past with the objectives of evaluating the performance of the Test Range and recommending ways of enhancing its facilities. Titles of reports giving some of the results of these prior studies are listed in Appendix I.

1.2 Objectives

The major objectives of the present study were two-fold:

1.) Determine the location of major reflection zones for the existing short and long test ranges and the effect of these reflections on antenna test measurements over the frequency range from 200 MHz to 2.0 GHz. Recommend techniques that can reduce the reflections and analyze the expected improvement in measurement accuracy obtained by each.

2.) Identify and analyze the site and instrumentation limitations to be anticipated in extending the Newport Test Range antenna measurement capability from 18 to 40 GHz.

The report includes some well-known results which are found in standard references, but these have been included here for completeness.

1
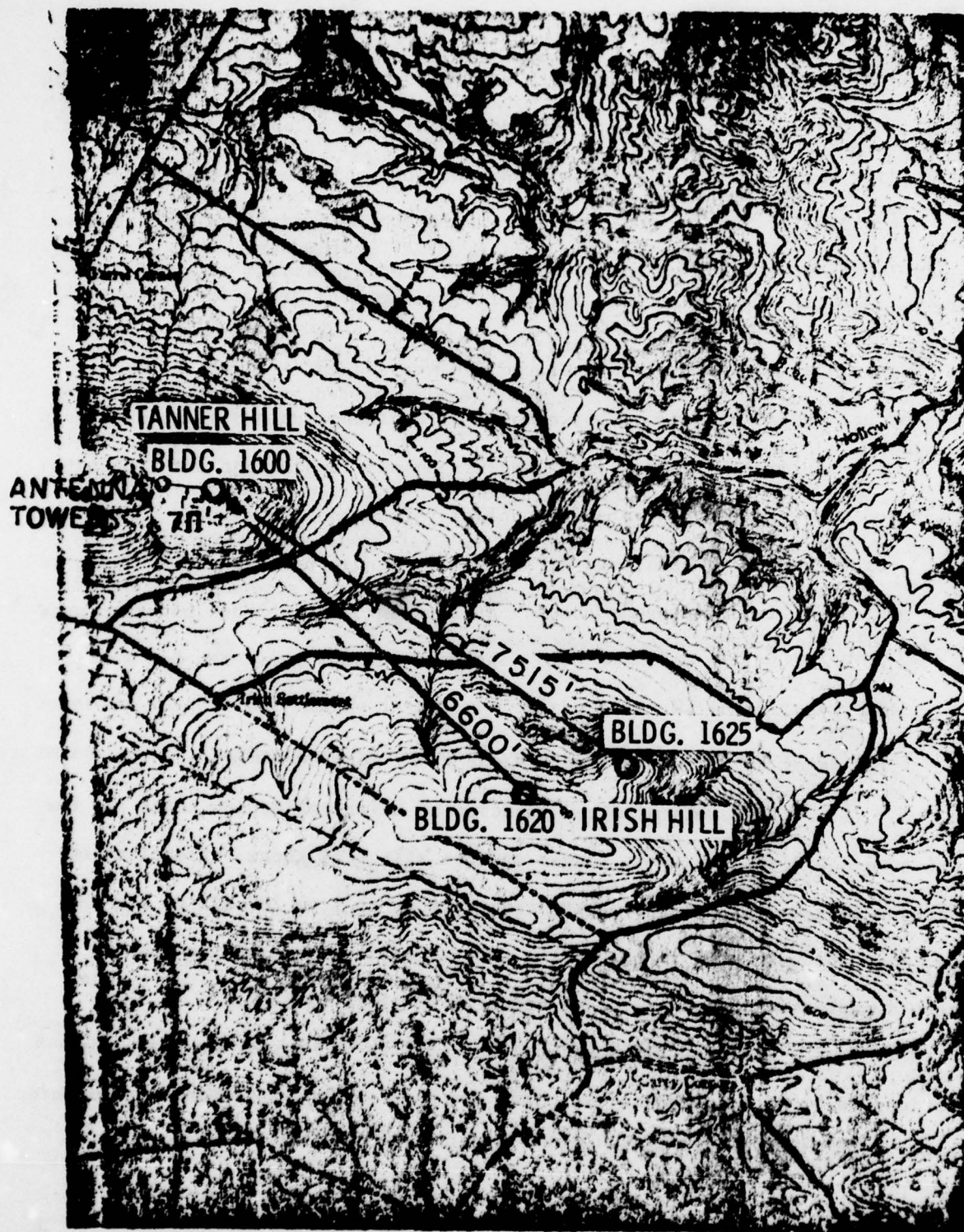
Figure 1. Topographic View of the RADC Antenna Test Site.

The experimental results and data included in this report were obtained by personnel of Rome Research Corporation (RRC) under the supervision of Mr. Eugene Nordell. This assistance is gratefully acknowledged.

2. REFLECTIONS

2.1 Statement of the Problem

A specific antenna pattern is usually obtained by employing the antenna as a receiving antenna. As a consequence of the Reciprocity Theorem[1], the transmitting and receiving patterns of an antenna are the same in a linear, passive, isotropic medium, if the illuminating field is a uniform plane wave. Major sources of disturbances in an otherwise uniform field frequently are reflections.

Any ponderable body such as the terrain, man-made structures, vegetation, etc. may give rise to reflections which disturb the field in the neighborhood of the test antenna.

2.2 Factors Affecting Reflection

1. _Terrain, obstacles._- The nature of the terrain or obstacles affects the resulting disturbance. If the terrain is smooth, the reflection appears to originate from a localized area or point. If the terrain is rough, there is more scattering and the effect is not easily localized. The terrain or structures becomes rough when the dimensions of its variations

---

[1]J.D. Kraus, _Antennas_. New York: McGraw-Hill Book Co., p. 252, 1950.

3

are comparable to the wavelength of the signal. It is more difficult to eliminate this source of disturbance than an apparent point source.

Obviously, vegetation and other natural growth which changes with the seasons as well as precipitation (rain and snow) affect reflections. Again, the exact nature of the effect is dependent on the wavelength of the signals.

2. _Antennas_. - The pattern of the illuminating antenna determines what portion of the surroundings is illuminated from which energy can be re-radiated. The aperture of the receiving (test) antenna determines what portion of this reradiated energy is intercepted. Furthermore, all but the simplest antennas are designed to operate in specified frequency ranges. When operated outside their prescribed frequency ranges, their radiating patterns and receiving apertures change. For example, the effective aperture, A_e, of an antenna is defined as the power W, in the terminating impedance of that antenna to the power density, P, of the incident wave:

$$A_e = \frac{W}{P}$$

It follows from this definition[2] that the maximum effective aperture of a lossless short dipole whose length, ℓ, is much less than the wavelength, λ, of the signal ($\ell << \lambda$) is:

$$A_{em} = 0.119\lambda^2.$$

Recall that in free space $f\lambda = c$ where f is the frequency of the signal and c is the velocity of light.

When antennas are operated outside the range for which designed, it

---

[2] J. D. Kraus, _Antennas_, New York: McGraw- Hill Book Co., Ch. 3, 1950.

4

is sometimes difficult to obtain even approximate expressions for their equivalent apertures.

3. _Aircraft mounted antennas_. - It is desired in these tests to obtain the characteristics of the antennas in their operating environment and not simply their free-space patterns. Consequently, it is important to isolate the reflections due to test facilities, terrain, and surrounding structures from those due to the aircraft structures on which the antennas will be mounted and which will form part of the antenna system.

By free-space pattern is meant the antenna pattern when an antenna is isolated in a vacuum and all ponderable bodies are an infinite distance from the given antenna.

2.3 Determination of Sources of Reflections

1. When a measured antenna pattern displays distinct peaks and nulls which are not predicted by its design, the cause is probably isolated sources of reflections.

The approximate location of the source of reflections can be determined as follows.

In Figure 2, it is assumed that the transmitted signal is a vertically-polarized, plane wave. Also, it is assumed that

$$R > \frac{2d^2}{\lambda} \tag{1}$$

where d is the aperture of the receiving antenna and

λ is the wavelength of the signal.

At the receiving site, suppose a probe is moved vertically and the

5

measured field is as shown in Figure 3. For purposes of analysis, the position of maximum measured field is labeled B and the position of minimum measured field is labeled C.

At position B, the sum of the reflected signal, V_R, plus the direct signal, V_D, is a maximum:

$$V_B = V_{max} = V_D + V_R = V_D(1 + \alpha)$$

Note that if V_D is given, V_R may be determined by specifying the boundary conditions at the point of reflection. Consequently, $V_R = \alpha V_D$ where α is a complex constant. This relation has been used in the above equation.

At C, the sum of the two signals is a minimum

$$V_C = V_{min} = V_D - V_R = V_D(1 - \alpha)$$

Incidently:

$$V_D = \frac{V_{max} + V_{min}}{2}, \tag{2}$$

$$\alpha = \frac{V_{max} - V_{min}}{V_{max} + V_{min}}. \tag{3}$$

If it is assumed that the path length of the direct signal is approximately the same for the receiving probe at points B and C, the path length of the reflected signal at point C must be $\lambda/2$ longer than that at point B. The wavelength of the signal is λ.

Therefore, referring to Figure 3:

$$\cos \theta = \frac{\lambda}{2(\Delta h)}. \tag{4}$$

6

Figure 2. Illustration of Idealized Point Reflection.

$$\cos\theta = \frac{\lambda}{2(\Delta h)}$$

Figure 3. Geometric Resolution of Direct and Reflected Signals.

In other words, by sighting at an angle θ from the receiving site, the location of the point of the reflection can be determined.

One technique used to eliminate the effects of a reflection is the installation of reflecting fences. This is illustrated in Figure 4.

Figure 4a shows a receiving antenna illuminated by the direct signal from a transmitting antenna plus a reflected signal. In Figure 4b, a reflecting fence of conducting material has been installed at the proper place and orientation which intercepts and redirects the reflected signal so that it does not interfere at the receiving site.

The use of reflecting fences has been the most successful method of eliminating reflections at the Newport Test Range. In fact, to test a particular antenna at a given frequency this technique is entirely satisfactory. In practice, however, the task becomes prohibitive if the range is used over a wide frequency range and for a variety of antennas because too many fences are required to neutralize all the points of reflection. As a compromise, two different ranges were used to cover the present frequency range of interest.

2.4 Results of Corrective Action *

There are four sites in operation at the Newport Test Range as indicated in Figure 1 on Tanner Hill and Irish Hill. Three ranges are available. Building 1600 on Tanner Hill is one terminus for each of the ranges. In addition, Buildings 1625, 1620, and an antenna tower 711 ft. west of building

---

*All data and figures labelled with an asterisk (*) were obtained by Rome Research Corporation (RRC) personnel. Details of their efforts are recorded in their monthly reports.
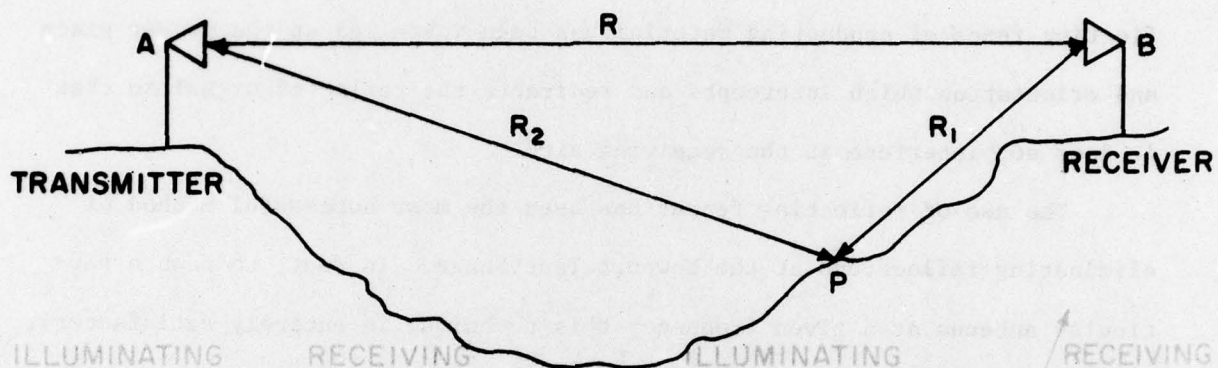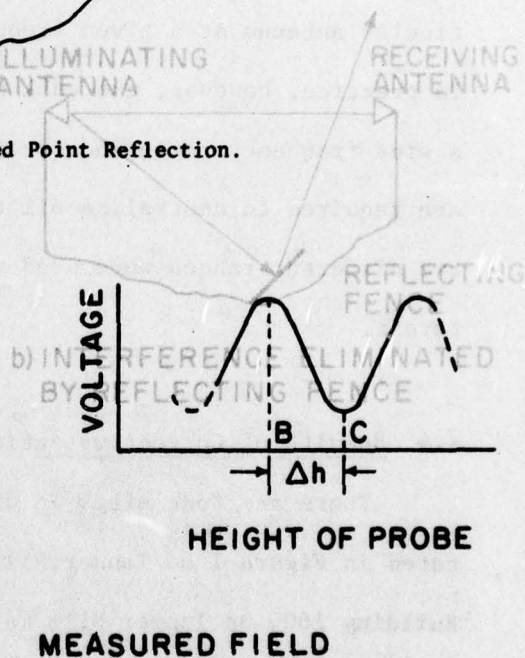
ILLUMINATING
ANTENNA

RECEIVING
ANTENNA

a) INTERFERING
REFLECTION

ILLUMINATING
ANTENNA

RECEIVING
ANTENNA

REFLECTING
FENCE

b) INTERFERENCE ELIMINATED
BY REFLECTING FENCE

Figure 4. Elimination of Reflections by Fences.

9

1600 on Tanner Hill each serve as the other site for separate ranges.

1. Range #2: Bldg. 1600, Tanner Hill - Bldg. 1625, Irish Hill

An elevation profile of the line-of-sight (LOS) terrain be-
tween buildings 1600 and 1625 is shown in Figure 5. In May, 1976, re-
flecting fences as indicated in Figure 6 were installed. The installation
consists of four fences, fifty feet long and four feet high. The wire is
one-half inch square mesh. The fences follow the contour of the terrain and
are inclined uphill to reflect the transmitted signals skyward. These
fences reduced reflections in the 200 MHz - 400 MHz frequency range but the
study was incomplete and more work is needed on this problem.

2. Section Range: Bldg. 1600, Tanner Hill-Bldg. 1620 Irish
Hill. - A profile sketch of the terrain between buildings 1600 and 1620 is
shown in Figure 7.

The field was probed as a function of elevation in the 0.5 GHz to
4.0 GHz range on Tanner Hill at the building 1600 site where it was illu-
minated by a parabolic dish antenna at the Irish Hill site. A typical plot
of the field is shown in Figure 8. Such a plot indicates reflections.

The length of vertical travel from top to bottom is 16 feet. If the
received signal were a uniform plane wave, the plot would be a constant.
The presence of approximately periodic peaks and nulls suggests that re-
flections are present as indicated in Figure 3. The fact that the ratio
of peaks to nulls is not constant over the entire plot suggests that more
than one reflection is present and that they do not all contribute signi-
ficantly to the received signal at all positions of the probe.

Further investigations revealed that when using available antennas,
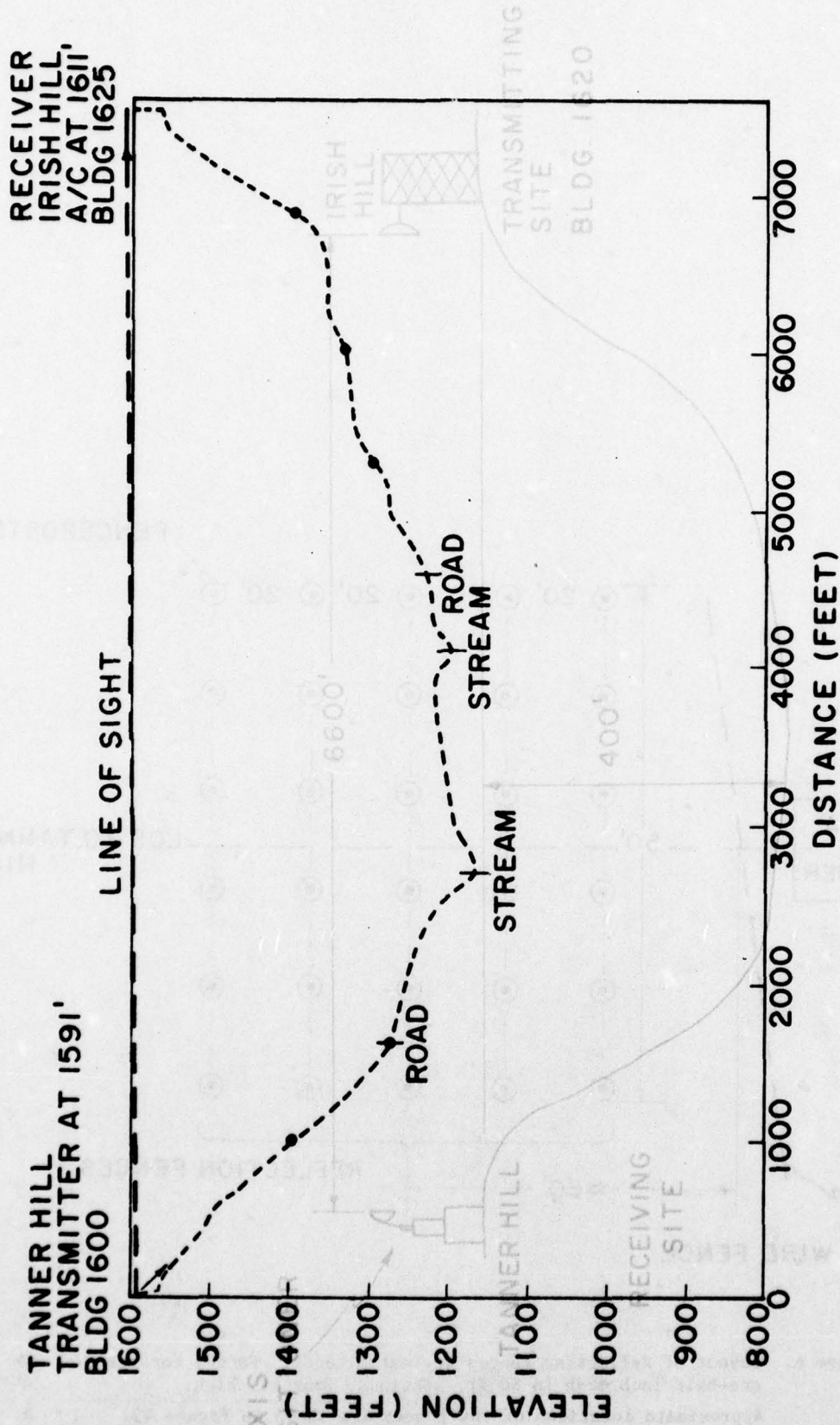
10

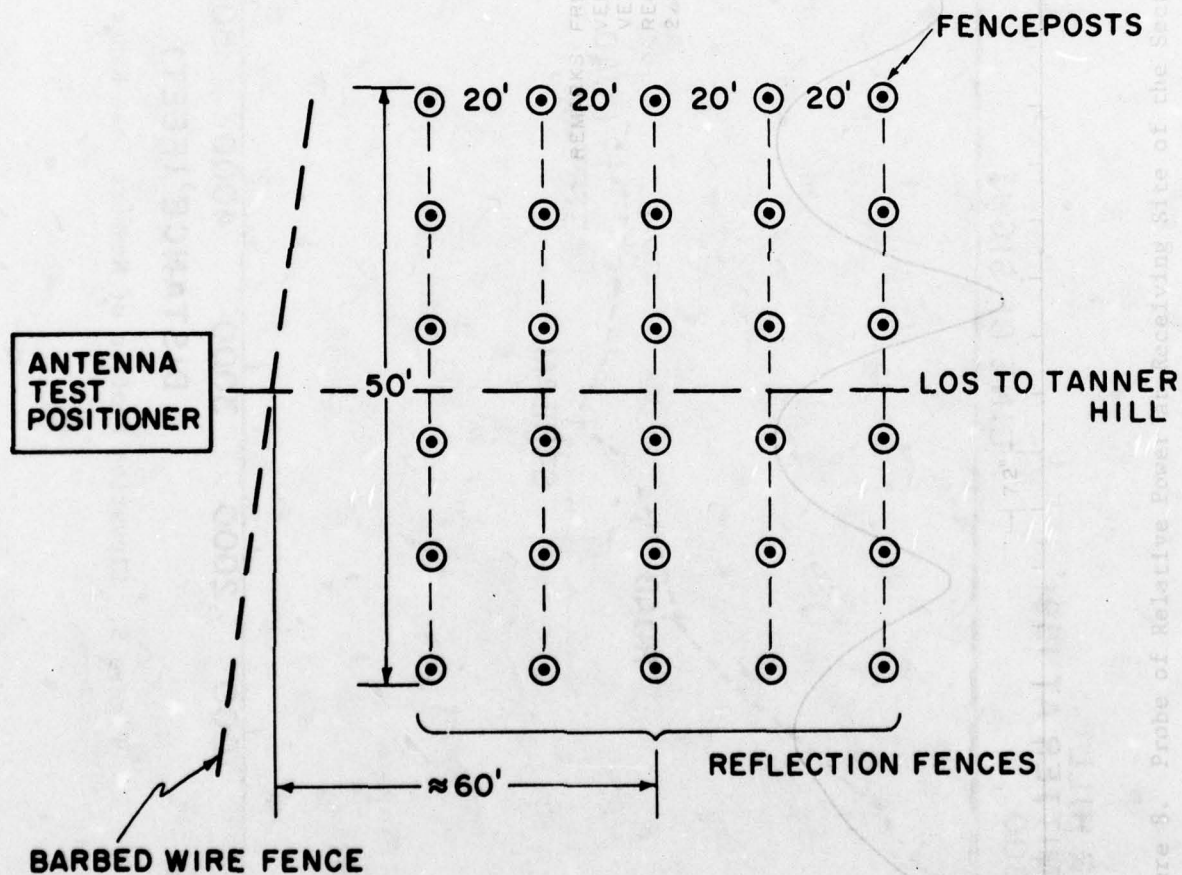Figure 5. Elevation Profile of Newport Test Range #2.

Figure 6. Layout of Reflecting Fences at Test Site #2. Fences consist of one-half inch mesh in 50 ft. sections, four ft. high.

Approximate locations of the fences are shown in Figure 22.

12

the total area of the terrain illuminated was too great to cover with re-
flecting fences when the Section Range was used for signals covering the
frequency range of 0.5 GHz to 4.0 GHz. Consequently, it was decided to
use this range only for 2.0 GHz to 4.0 GHz at present.

After further study, reflecting fences were installed as shown in
Figure 9. A copy of two plots in Figures 10 and 11 show the reductions in
reflections. Figure 10 is a copy of the vertical pattern recorded before
any fences were erected. Notice that one sidelobe is only 3 db below the
main beam and the plot is highly unsymmetrical. Figure 11 shows the plot
after the reflecting fences were installed. Here the pattern more closely
approximates the free space pattern with successive sidelobes decreasing
as predicted.

3. Short Range Corrections. - In checking the Section Range (Bldg
1600-Bldg 1620) it was found that the available antennas would not perform
satisfactorily over the desired frequency range of 0.5 GHz to 2.0 GHz. Re-
flecting fences were installed which gave satisfactory results in the range
of 2.0 GHz to 4.0 GHz as described in the above section. However, below
2.0 GHz the beam width of the antennas was so great that a large area of
terrain was illuminated which resulted in interfering signals at the an-
tenna site on Bldg. 1600. Installing additional fences was too big an
effort. Changing antennas during a test was too unwieldly and time con-
suming. Consequently, it was decided to use the so-called Short Range for
measurements in the 0.5 GHz to 2.0 GHz frequency range.

A sketch of this range is shown in Figure 12a and Figure 12b.

Figures 13 and 14 show a probe of the field (hopefully uniform) taken

Figure 7. Profile Sketch and Section Range.

IRISH HILL

TRANSMITTING SITE BLDG. 1620

6600'

400'

TANNER HILL

RECEIVING SITE

3 AXIS POSITIONER

13

REMARKS: FREQUENCY-1.0 GHz
VERTICAL POLARIZATION
VERTICAL SWEEP (16')
RECEIVING ANTENNA-LOG PERIODIC
2/8/77

TOP

50'

60'

60'

90'

145'

BOTTOM

7.2"

RELATIVE POWER (dB)

8 10 12 14 16 18 20 22 24 26 28 30

75'
32'
82'
82'
82'

Note: In initial installation, fences were four feet high.
In final installation, fences were seven and one-
half feet high (eight-feet fencing at twenty degree
angle of repose).
Fencing consists of one-quarter inch mesh wire.

100'

BLDG 1600

LEGEND

INSTALLED WIRE FENCE
PORTABLE FENCE
SECTIONS FROM

Figure 8. Probe of Relative Power at Receiving Site of the Section Range (*Measurements by RRC).

Figure 9. Initial Reflecting Fence Installation, Receiving Range

14

the total area of the terrain illuminated was too great to cover with reflecting fences when the Section Range was used for signals covering the frequency range of 0.5 GHz to 4.0 GHz. Consequently, it was decided to use this range only for 2.0 GHz to 4.0 GHz at present.

After further study, reflecting fences were installed as shown in Figure 9. A copy of two plots in Figures 10 and 11 show the reductions in reflections. Figure 10 is a copy of the vertical pattern recorded before any fences were erected. Notice that one sidelobe is only 8 db below the main beam and the plot is highly unsymmetrical. Figure 11 shows the plot after the reflecting fences were installed. Here the pattern more closely approximates the free space pattern with successive sidelobes decreasing as predicted.

3. <u>Short Range Corrections</u>. - In checking the Section Range (Bldg 1600-Bldg 1620) it was found that the available antennas would not perform satisfactorily over the desired frequency range of 0.5 GHz to 4.0 GHz. Reflecting fences were installed which gave satisfactory results in the range of 2.0 GHz to 4.0 GHz as described in the above section. However, below 2.0 GHz the beam width of the antennas was so great that a large area of terrain was illuminated which resulted in interfering signals at the antenna site on Bldg. 1600. Installing additional fences was too big an effort. Changing antennas during a test was too unwieldly and time consuming. Consequently, it was decided to use the so-called Short Range for measurements in the 0.5 GHz to 2.0 GHz frequency range.

A sketch of this range is shown in Figure 12a and Figure 12b.

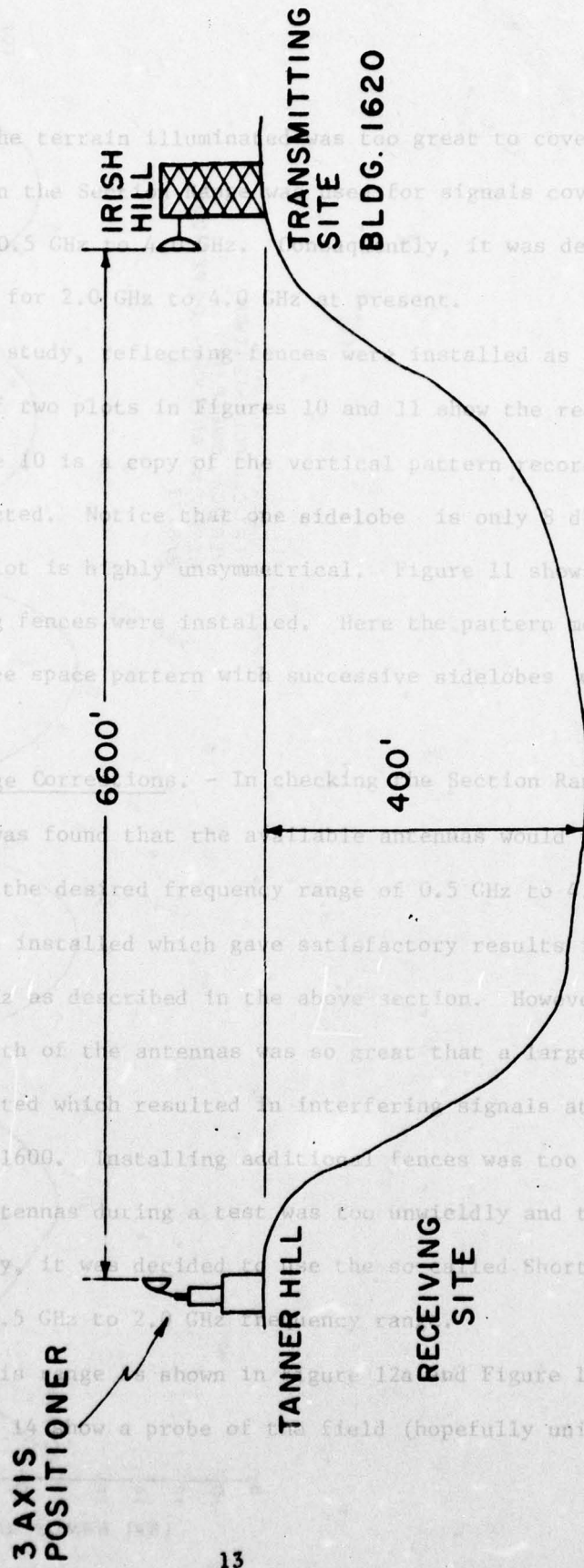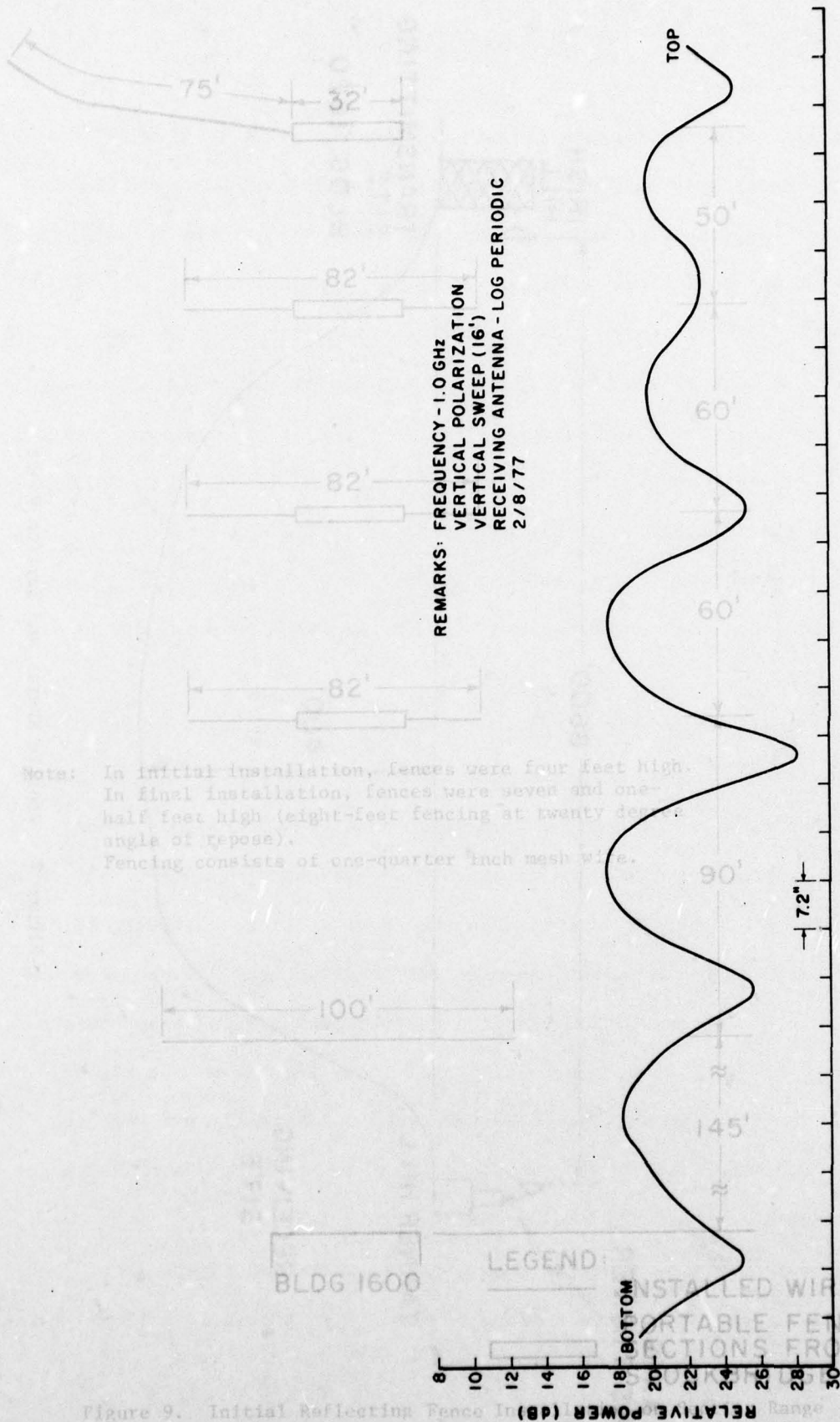Figures 13 and 14 show a probe of the field (hopefully uniform) taken
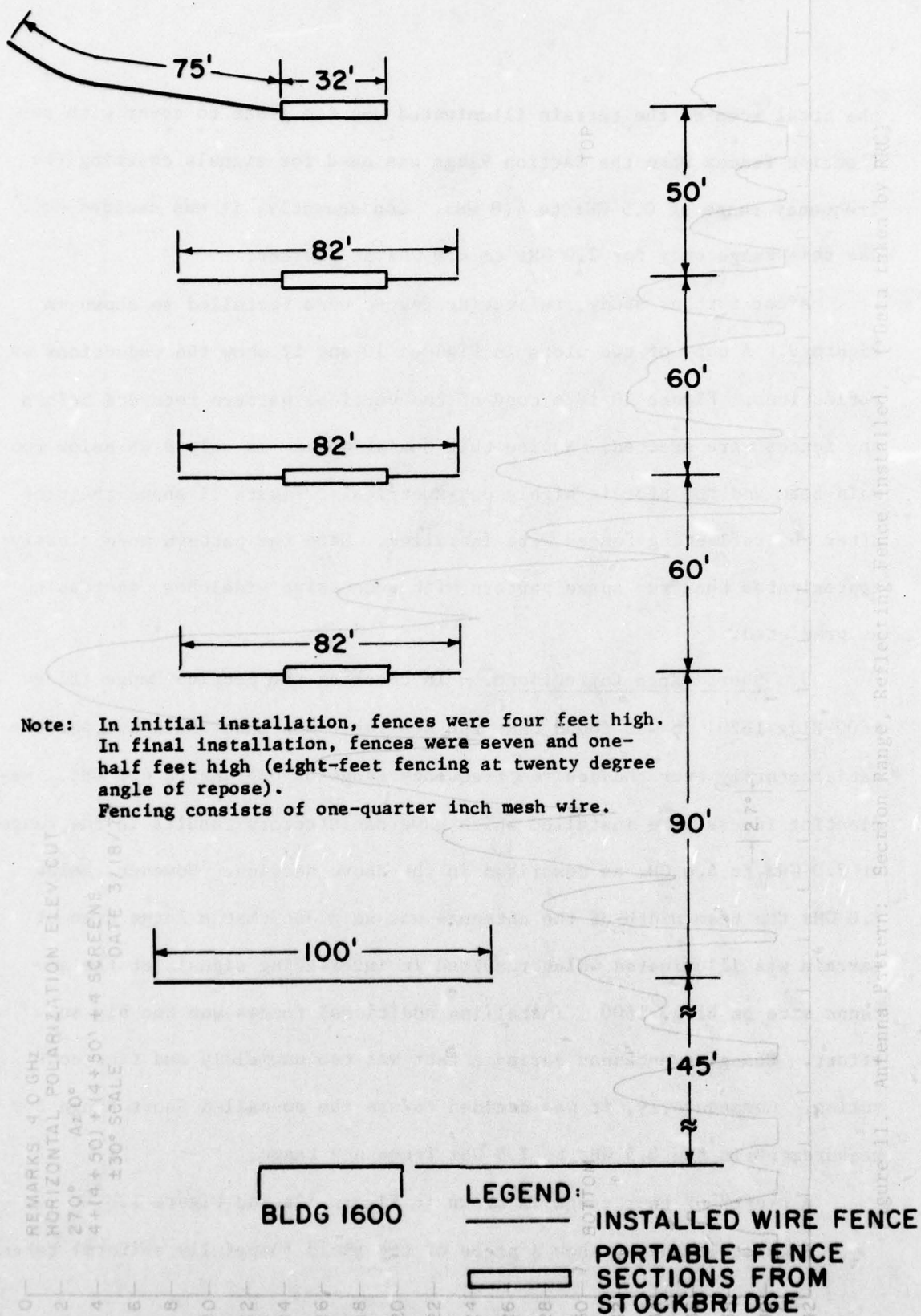
15

```
                    ┌──────────────────────────┐
                   ╱│           TOP            │
         ╱────────  │                          │
        ╱    75'    │▼  32'  ▲                 ├─ 50'
       ◀───────────▶│ ┌────┐                   │
                    │ └────┘                   │
                    │                          ├─ 60'
        ◀──── 82' ──▶                          │
         ┌──────────┐                          │
         └──────────┘                          ├─ 60'
                    │                          │
        ◀──── 82' ──▶                          │
         ┌──────────┐                          ├─ 90'
         └──────────┘                          │
```

Note: In initial installation, fences were four feet high.
In final installation, fences were seven and one-
half feet high (eight-feet fencing at twenty degree
angle of repose).
Fencing consists of one-quarter inch mesh wire.

```
        ◀──── 82' ──▶                          ├─ 90'
         ┌──────────┐                          │
         └──────────┘                          │
                                               │
        ◀──────── 100' ───────▶                ├─ 145'
         ──────────────────────                │
```

```
┌───────────────┐   LEGEND:
│   BLDG 1600   │   ───────────  INSTALLED WIRE FENCE
└───────────────┘
                    ┌──────────┐  PORTABLE FENCE
                    └──────────┘  SECTIONS FROM
                                  STOCKBRIDGE
```

Figure 9. Initial Reflecting Fence Installation on Section Range

16

REMARKS: 6' DISH
Az ⊘ 359°
HOR. POL. EL. PATTERN
4.0 GHz
XMIT ANT. 28'
BEAM DEPRESS
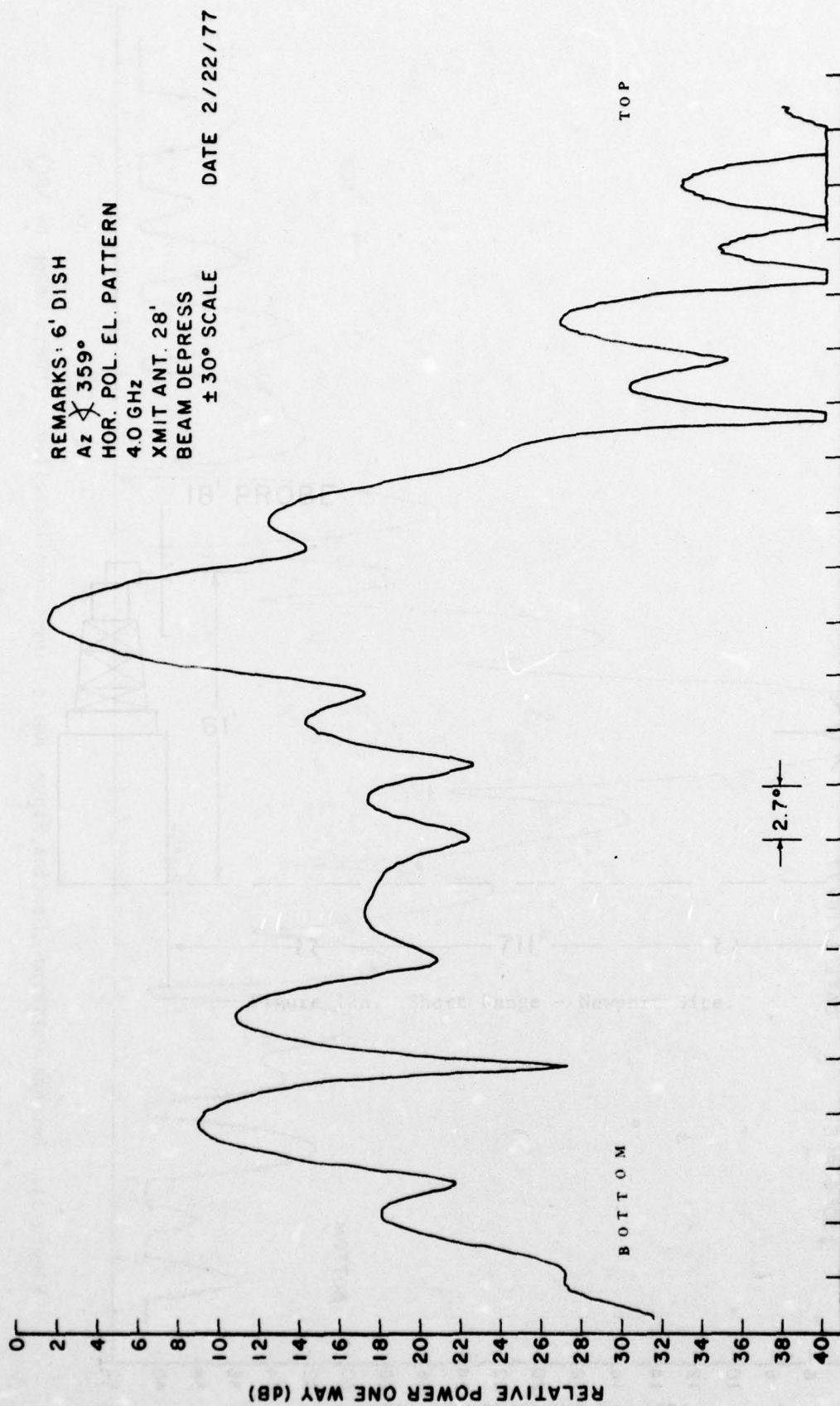±30° SCALE   DATE 2/22/77

Figure 10.   Antenna Pattern: Section Range, no Reflecting Fences. (*Data taken by RRC)
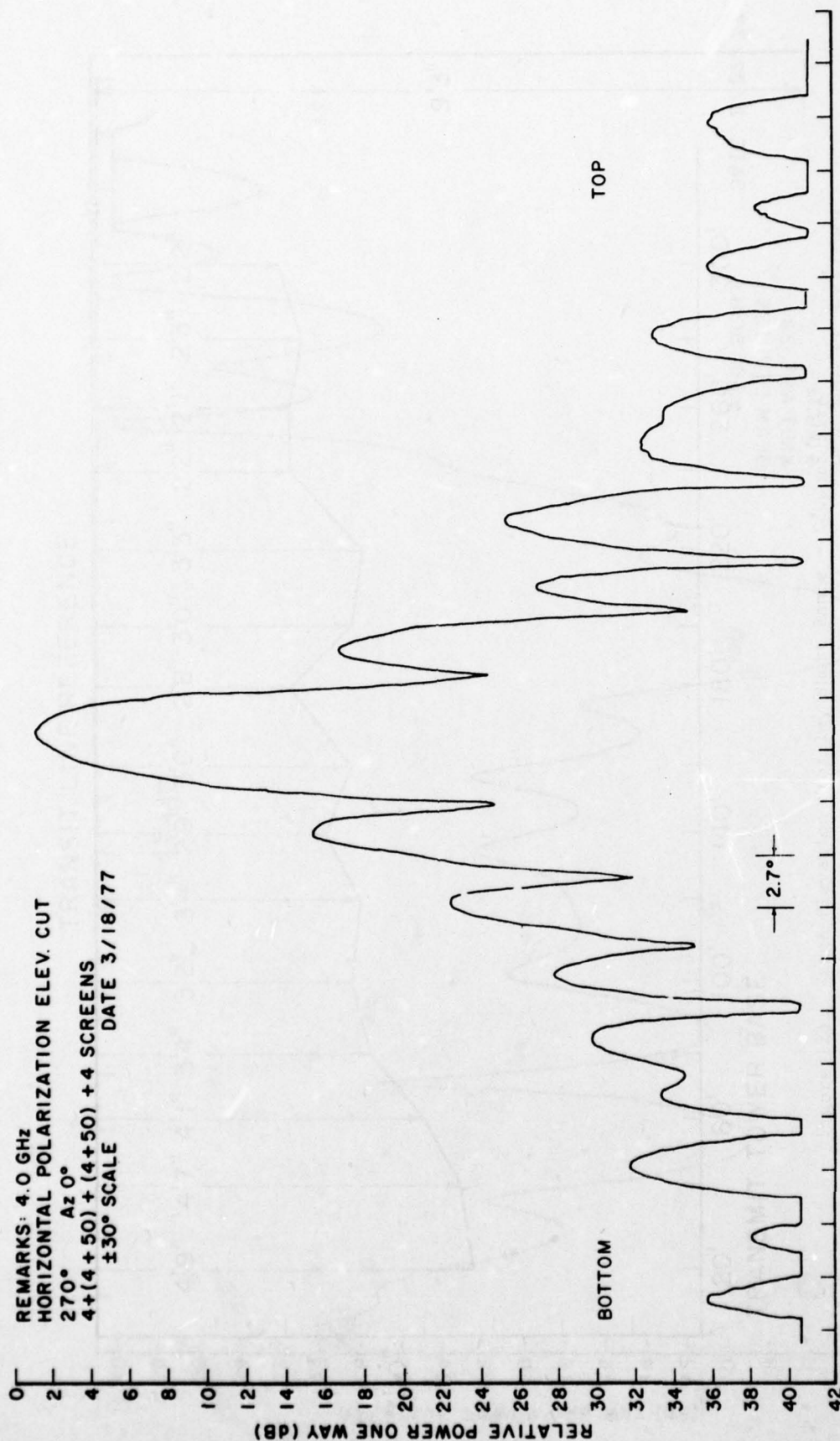
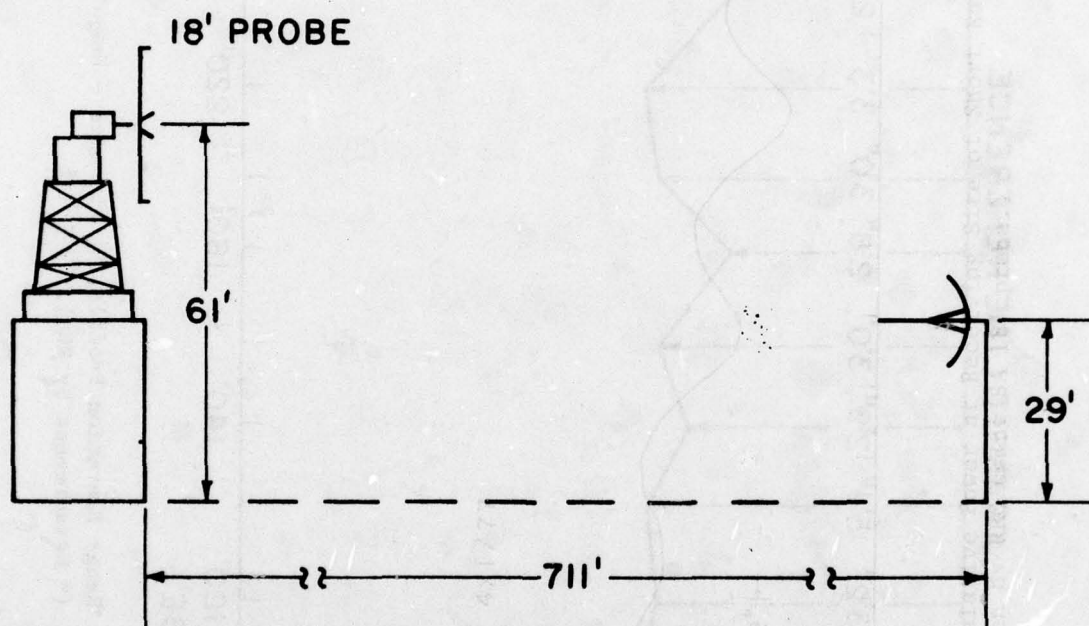Figure 11. Antenna Pattern: Section Range, Reflecting Fence Installed. (*Data taken by RRC)

18

18' PROBE

61'

29'

711'

Figure 12a. Short Range - Newport Site.
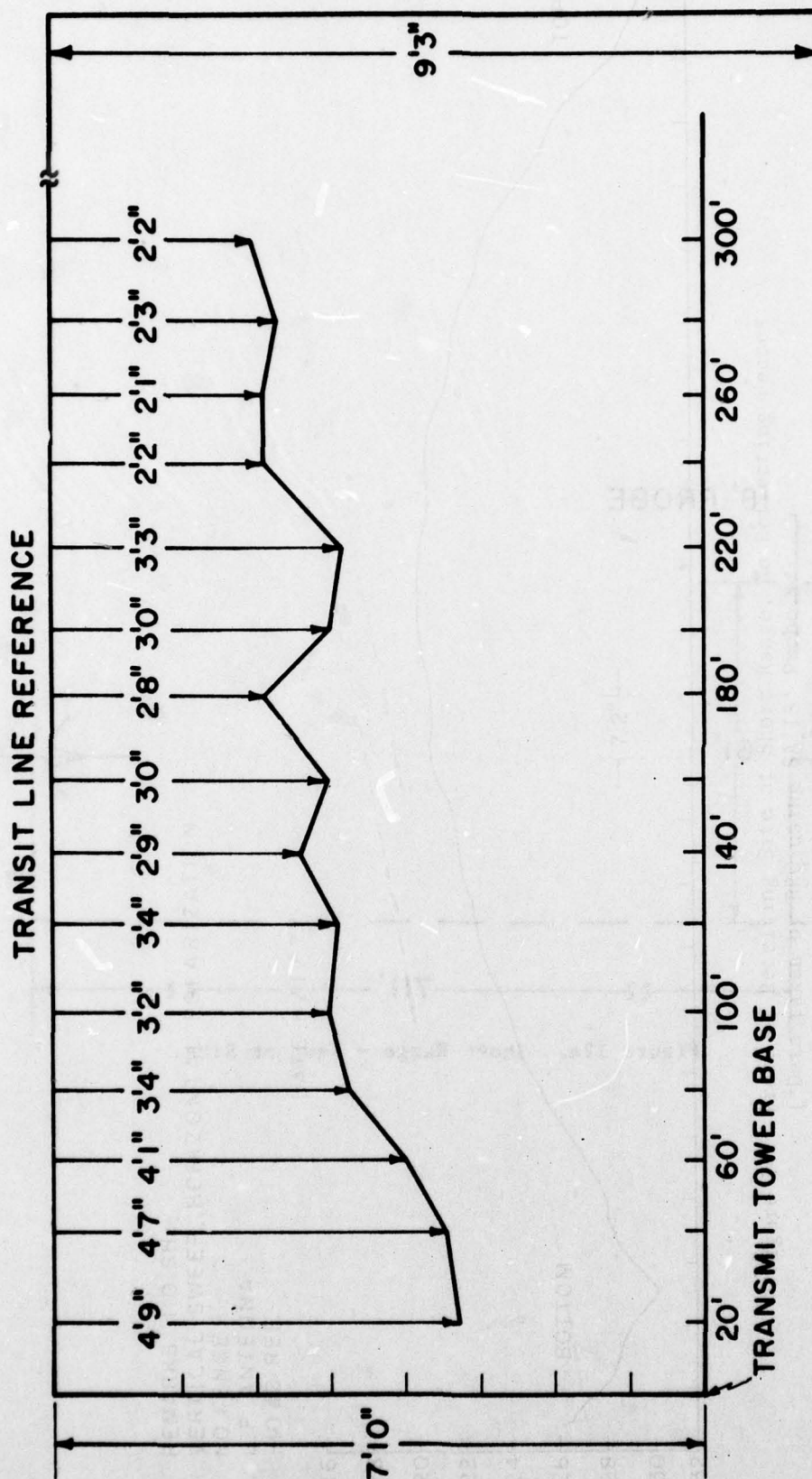
Figure 12b. Range Elevation Profile, Short Range - Newport Site
(* Measurement by RRC).

20

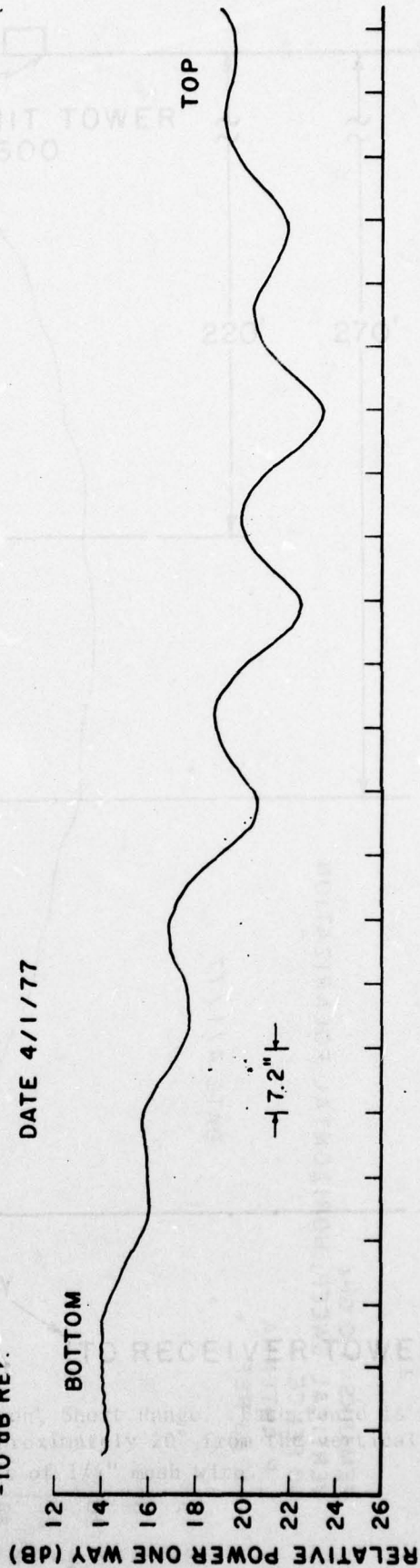Figure 13: Probe of Relative Power at Receiving Site of Short Range, No Reflecting Fences.
(*Data taken by RRC using SA 18' probe.)

REMARKS: 1.0 GHz
VERTICAL SWEEP, HORIZONTAL POLARIZATION
NO FENCE
L.P. ANTENNA
-10 dB REF.

DATE 4/1/77
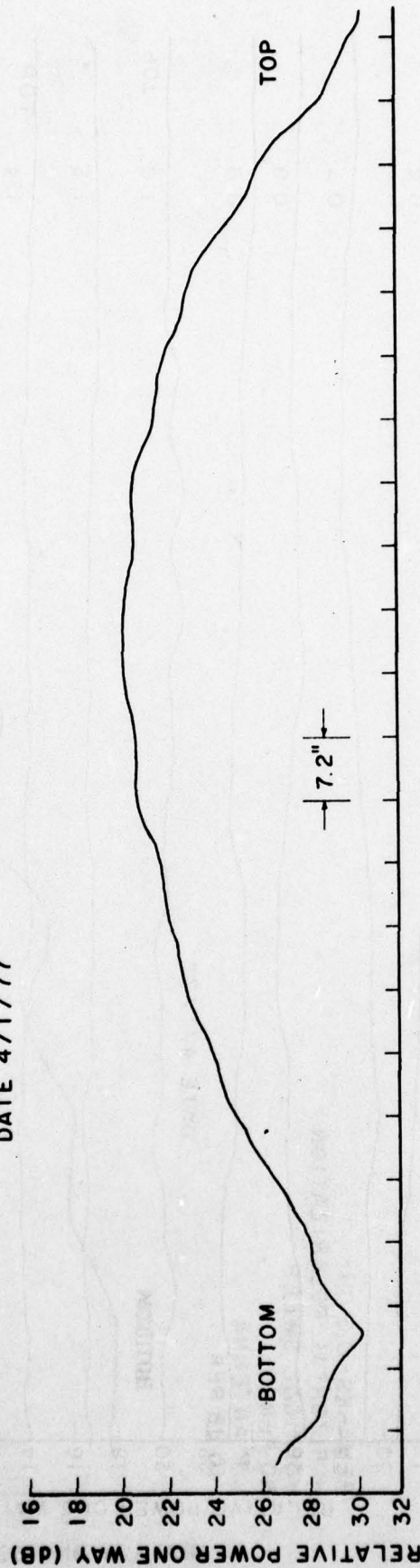
Figure 14. Probe of Receiving Site at Short Range, No Reflecting Fences
(*Data taken by RRC using SA 18' Probe.)

RELATIVE POWER ONE WAY (dB)

7.2"

TOP

BOTTOM
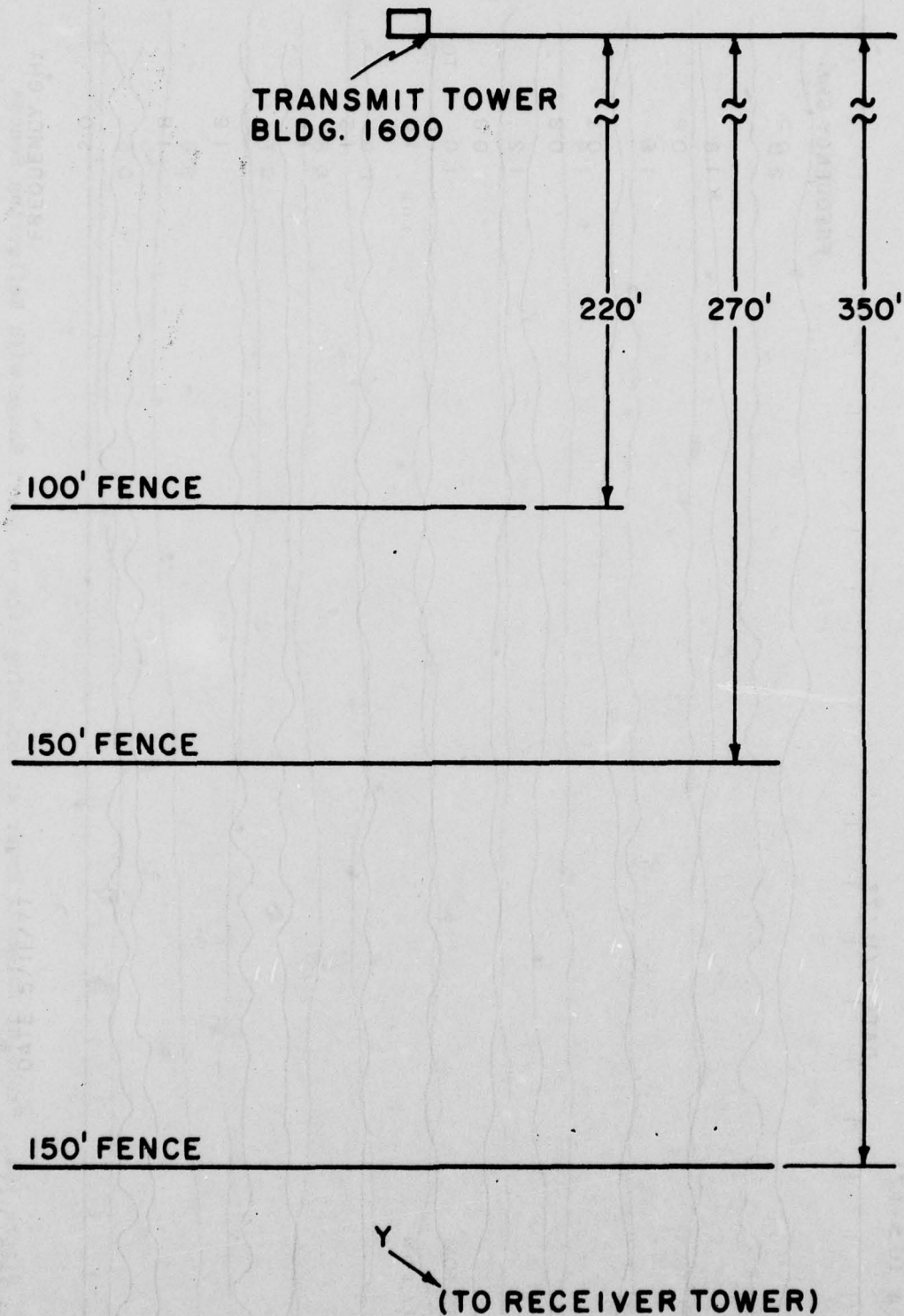
Figure 15. Fence Configuration, Short Range. Each fence is 8 feet high and sloped at approximately 2[?] from the vertical. The fences consist of 1/4" mesh w[?].

Figure 16a. Probe of Relative Power at Receiving Site of Short Range with Reflecting Fences Installed. (*Data taken by RRC).

24

REMARKS: 2.0 - 0.5 GHz
HORIZ. POLARIZATION VERTICAL SWEEP (16')
FINAL CUT
L.P.-S.A. (0.5-1.7)   DATE 5/11/77

FREQUENCY GHz

2.0

1.8

1.6

1.4

1.2

TOP   1.0

0.9

0.8

0.7

0.6

0.5

BOTTOM

RELATIVE POWER ONE WAY (dB)

0 2 4 6 8 10 12 14 16 18 20 22 24 26 28 30 32 34 36 38

Figure 16b. Probe of Relative Power at Receiving Site of Short Range with Reflecting Fences
Installed. (*Data taken by RRC).

25

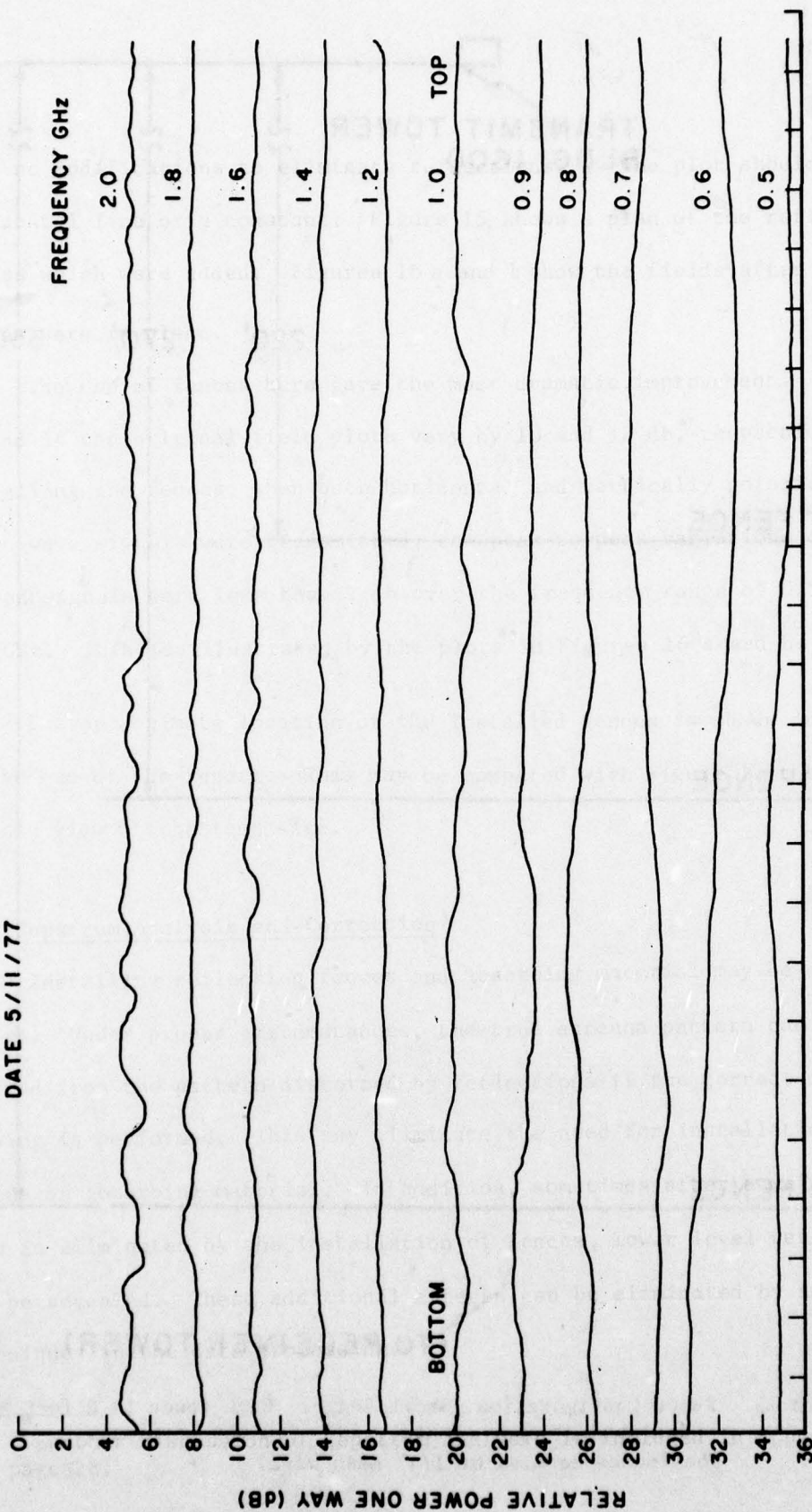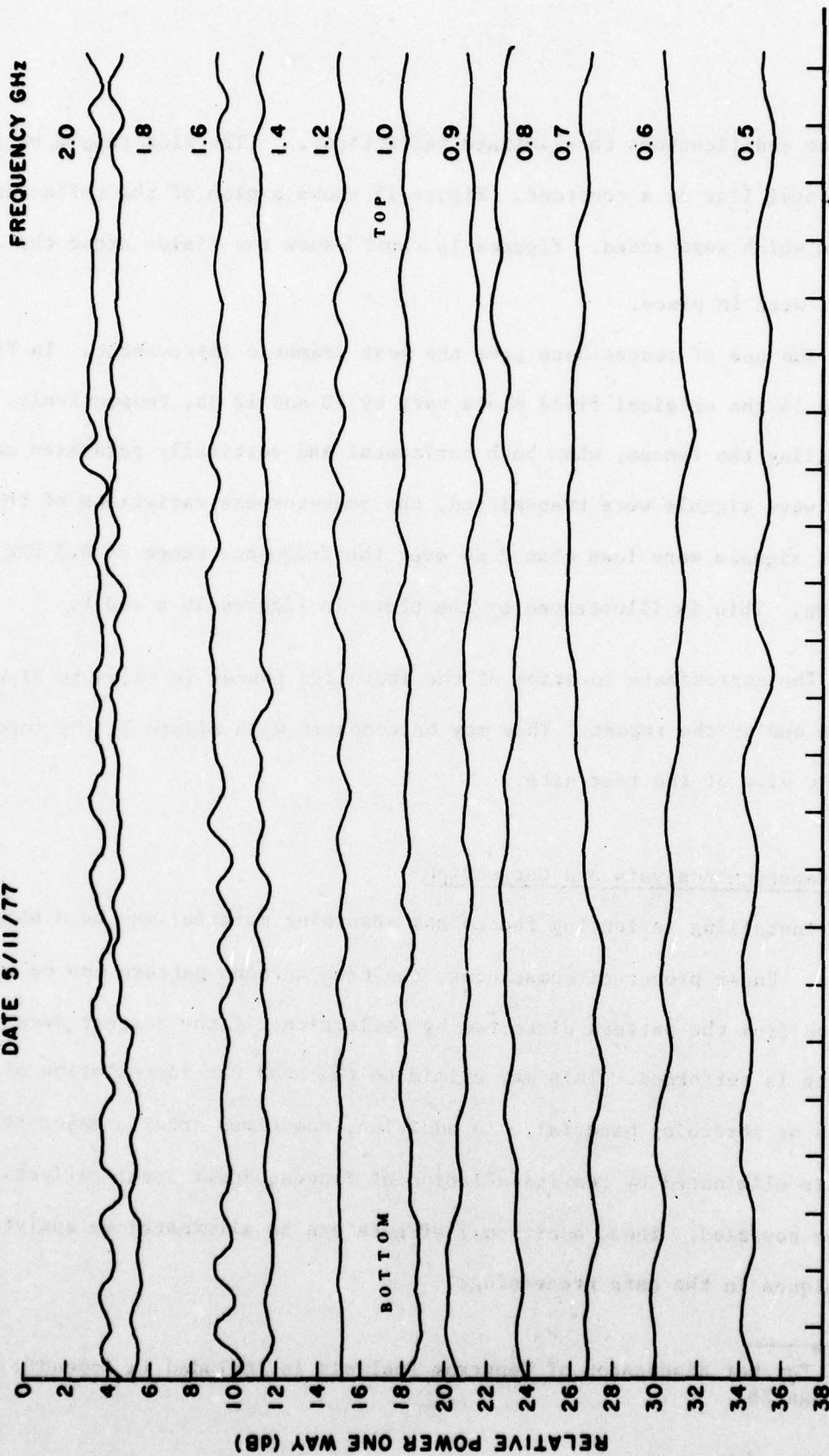with no modifications to eliminate reflections. The plot should be a horizontal line or a constant. Figure 15 shows a plan of the reflecting fences which were added. Figures 16 a and b show the fields after the fences were in place.

The use of fences here gave the most dramatic improvement. In Figures 13 and 14 the original field plots vary by 10 and 12 db, respectively. After installing the fences, when both horizontal and vertically polarized uniform plane wave signals were transmitted, the peak-to-peak variations of the received signals were less than 2 db over the frequency range of 0.5 GHz to 2.0 GHz. This is illustrated by the plots in Figures 16 a and b.

The approximate location of the installed fences is shown in Figure 22 at the end of the report. This may be compared with Figure 1, the topographic view of the test site.

2.5 Cepstrum Analysis and Correction*

Installing reflecting fences and absorbing material may be a major effort. Under proper circumstances, the true antenna pattern can be extracted from the pattern distorted by reflections if the correct data processing is performed. This may eliminate the need for installation of fences or absorbing material. In addition, sometimes after a major reflection is eliminated by the installation of fences, lower level reflections may be revealed. These additional effects can be eliminated by analytical techniques in the data processing.

----

    *
    Further discussion of Cepstrum Analysis is included in Appendix
II, page 28.

26

The basis for this analytical technique is the cepstrum analysis[*] which will now be developed.

In Figure 17, let

$x(\theta)$ = measured radiation pattern due to the direct
signal along path R only   (5)

$\alpha x(\theta-\theta_0)$ = measured pattern due to the multipath signal

along $(R_1 + R_2)$.   (6)

α is a complex reflection factor and θ_0 is the angle between directions R and R_2.

The actual measured pattern is the sum of the two above signals or

$$y(\theta) = x(\theta) + \alpha x(\theta - \theta_0) \qquad (7)$$

Usually, $|\alpha| < 1$ and $\theta_0 > 0$.

If α and θ_0 can be determined, and if $y(\theta)$ is measured, Eq. (7) can be solved to yield $x(\theta)$, the true antenna pattern. For simplicity, only one reflection is considered but the technique can be extended to include several reflections. The solution of Equation (7) can be implemented also by hardware as indicated in Figure 18. Note that the input is the total received signal and has been designated $y(\theta)$. The output is the desired antenna pattern and has been designated $x(\theta)$. By inspection of the circuit diagram in Figure 18:

$$x(\theta) = y(\theta) - \alpha x(\theta-\theta_0).$$

The quantities α and θ_0 can be determined by the techniques already in use to determine the locations of the sources of reflections.

---

*Bogert, Healy, Tukey, "The Quefrency Analysis of Time Series for Echoes," Proc. Sym. on Time Series Analysis, M. Rosenblatt (ed.), J. Wiley, 1963.
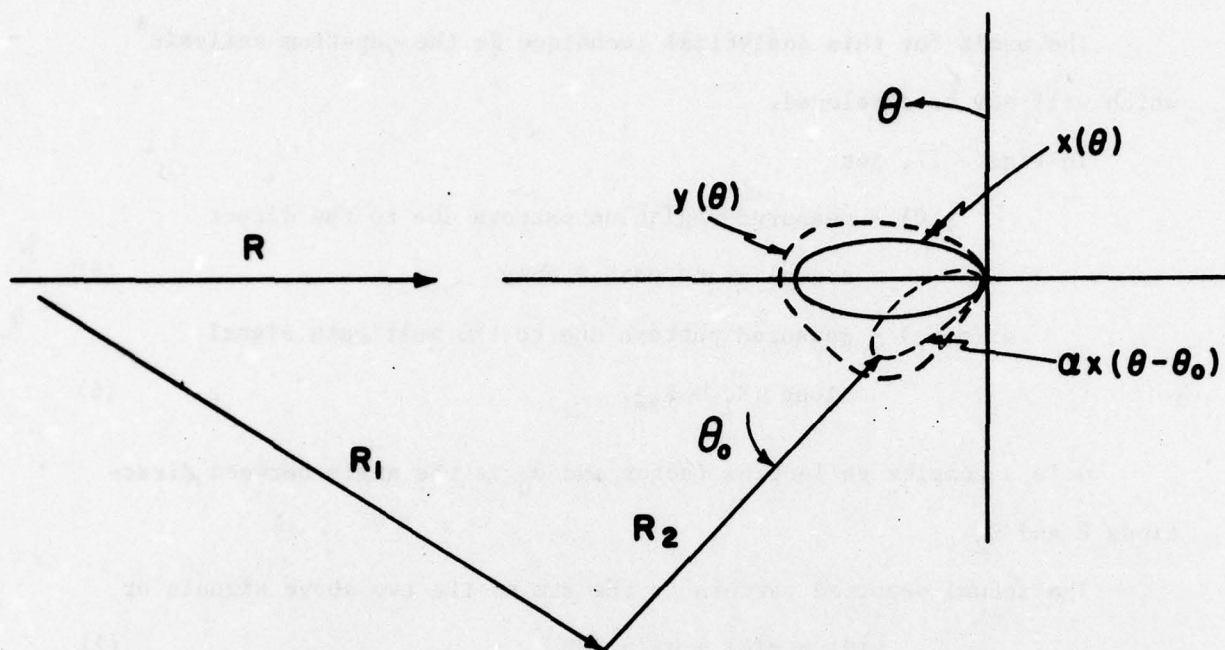
RECORDED FIELD STRENGTH PLOT, $y(\theta) = x(\theta) + \alpha x(\theta - \theta_0)$.

Figure 17.

$z^{-\theta_0}$ REPRESENTS A
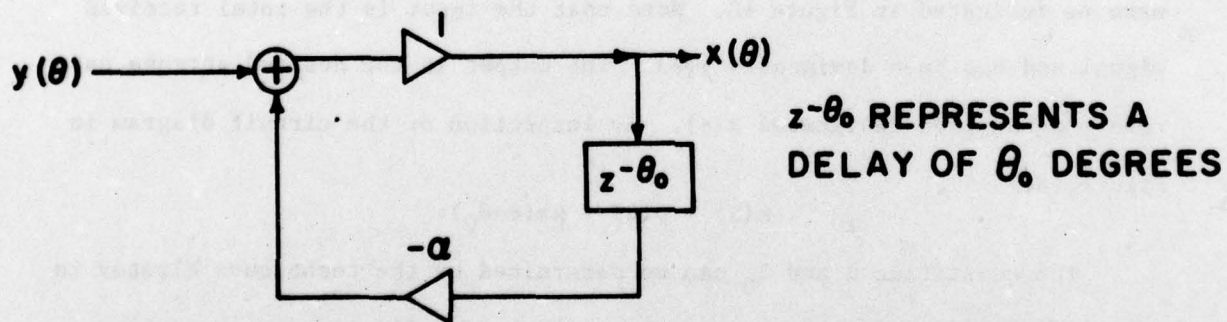DELAY OF θ_0 DEGREES

Figure 18.   Implementation of $y(\theta) = x(\theta) + \alpha x(\theta - \theta_0)$

28

However, they also can be determined by the method of cepstrum analysis. Potentially, this will result in an enormous savings in time and effort. Furthermore, the circuit of Figure 18 may be replaced by a direct computation. In Equation (7) if α and θ_0 are known and $y(\theta)$ is measured, $x(\theta)$ can be determined by

$$x(\theta) = y(\theta) - \alpha x(\theta - \theta_0) \tag{8}$$

This is developed in what follows.

2.5.1 Cepstrum analysis- In this analysis it is assumed that the pattern $x(\theta)$ of the test antenna is given and that the illuminating source is a uniform plane wave. If there is a single reflection, the measured signal is

$$y(\theta) = x(\theta) + \alpha x(\theta - \theta_0); \qquad |\alpha| < 1, \theta_0 > 0. \tag{9}$$

Define the Fourier transform of $x(\theta)$ as

$$F_x(\omega) = \int_{-\infty}^{\infty} x(\theta) \epsilon^{-j\omega\theta} d\theta = F(x); \qquad \omega = 2\pi f. \tag{10}$$

and

$$L_x(\omega) = \ln(F(\omega)) \text{ which is the logarithm of } F(\omega). \tag{11}$$

Then the following processing is performed on $y(\theta)$.

$$F_y(\omega) = \int_{-\infty}^{+\infty} [x(\theta) + \alpha x(\theta - \theta_0)] \epsilon^{-j\omega\theta} d\theta \tag{12}$$

$$= [1 + \alpha \epsilon^{-j\omega\theta_0}] F_x(\omega) \tag{13}$$

$$L_y(\omega) = \ln(F_y(\omega)) = \ln(1 + \alpha \epsilon^{-j\omega\theta_0}) + \ln(F_x(\omega)). \tag{14}$$

29

$$y(n) = x(n) \dotplus \alpha x(n-n_0); \quad \theta(n-1)-\theta(n)= \frac{\Pi}{8}; \quad \alpha = 1/2, \; n_0 = 2$$
$$x(n) = y(n) - 1/2 \, x(n-2)$$

TABLE 3

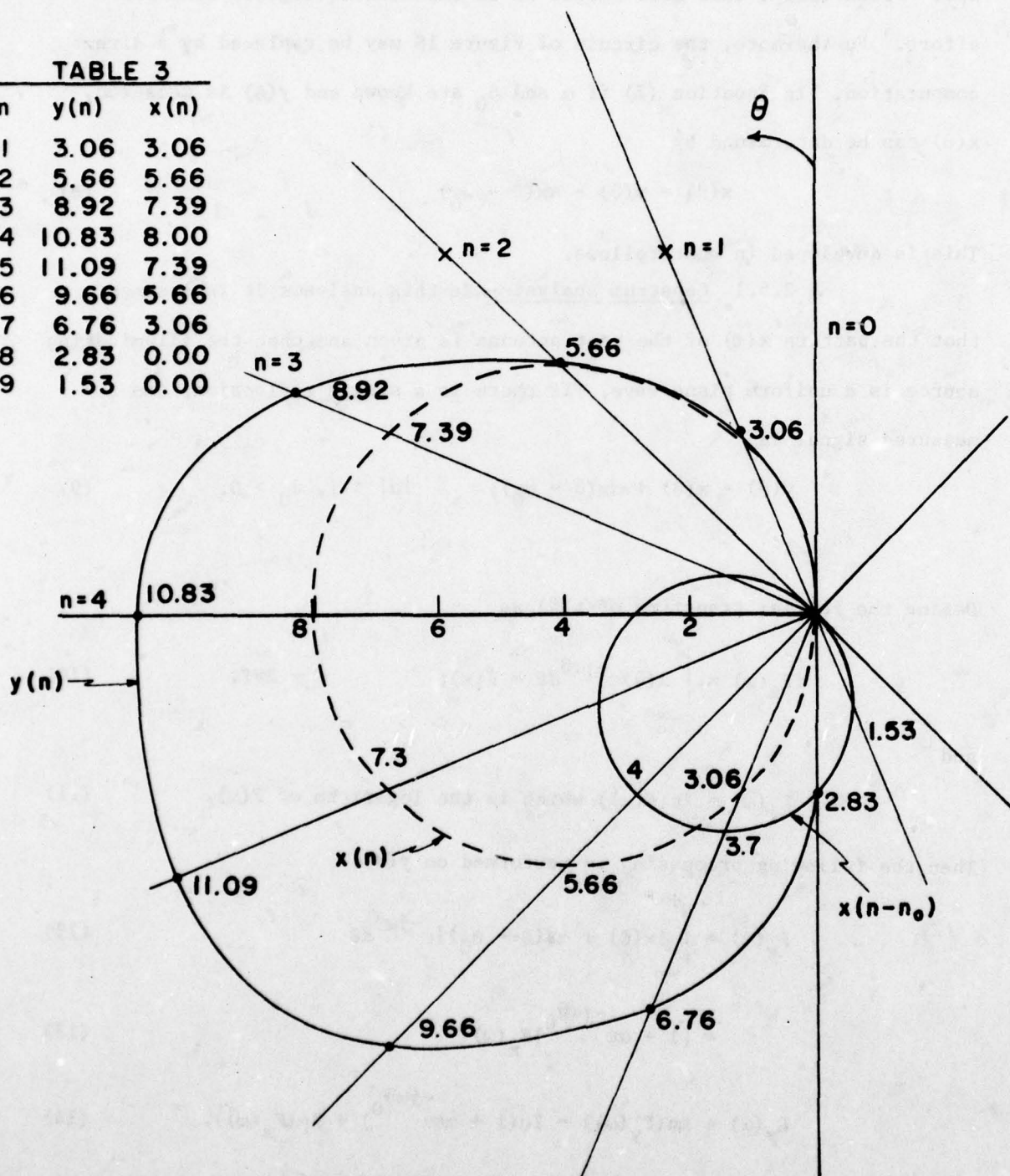| n	y(n)	x(n)
1	3.06	3.06
2	5.66	5.66
3	8.92	7.39
4	10.83	8.00
5	11.09	7.39
6	9.66	5.66
7	6.76	3.06
8	2.83	0.00
9	1.53	0.00

Figure 19. Application of Cepstrum Analysis to Antenna Pattern Determination.

If $|\alpha| \ll 1$,

$$L_y(\omega) \simeq \alpha \varepsilon^{-j\omega\theta_0} + \ell n(F_x(\omega)) \qquad (15)$$

Finally, taking the inverse Fourier transform of (15) yields:

$$F^{-1}(L_y(\omega)) = \frac{1}{2\pi} \int_{-\infty}^{+\infty} L_y(\omega) \varepsilon^{j\omega\theta'} d\omega \qquad (16)$$

$$= \frac{1}{2\pi} \int_{-\infty}^{+\infty} [\alpha\varepsilon^{-j\omega\theta_0} + \ell nF_x(\omega)]\varepsilon^{j\omega\theta'} d\omega \qquad (17)$$

$$= \alpha\delta(\theta' - \theta_0) + F^{-1}L_x(\omega) ; \begin{array}{l} \delta(\theta)=\text{Dirac Delta} \\ \qquad \text{Function} \\ =1, \ \theta=0 \\ =0, \ \text{otherwise} \end{array} \qquad (18)$$

or

$$\alpha\delta(\theta' - \theta_0) = F^{-1}(L_y(\omega)) - F^{-1}(L_x(\omega)) \qquad (19)$$

The quantity $F^{-1}(L_y(\omega))$ determined by equation (16) is called the cepstrum of $y(\theta)$. It is the inverse transform of the logarithm of the direct Fourier transform of $y(\theta)$. Because of the step of taking the logarithm of $F_y(\omega)$, the domain of the independent variable of Equation (16) is not θ; it has been named the cepstrum. However, because of the general relationship log AB = log A + log B, the value of α and θ_0 can be obtained from the cepstrum of a multipath signal (or function) if the undistorted value of the signal is known.

Notice that this inverse transform includes an impulse (or Delta Function) which is delayed θ_0 and of amplitude α which allows determination of these two quantities.

Repeating, knowing α and θ_0, the pattern $x(\theta)$ of an unknown antenna

31

can be obtained by computation using Equation (8) or processing with the hardware of Figure 18.

Equation (19) reveals why we require the field strength plot of an antenna whose free space pattern is known. Observe that magnitude and delay of the reflection equals the _cepstrum_ of the received data minus the cepstrum of the free space or undistorted pattern.

Equation (15) assumes $|\alpha| \ll 1$. If this is not true, other impulses will appear in the solution, but they will have values of $\frac{(\alpha)^n}{n!} \delta(\theta - n\theta_0)$ and can be recognized. Impulses due to other reflections which appear will not be so related. Again, $\delta(\theta) = 1$, $\theta = 0$ and $\delta(\theta) = 0$, otherwise.

Finally, Equation (8) is a first-order difference equation and to obtain a unique solution, one initial value is required.

An example of the application of the technique follows in the next section.

2.5.2 _Cepstrum Processing_ – The application of cepstrum processing can be illustrated by an example.

Let the solid line in Figure 19 represent a recorded field strength plot. Furthermore, suppose that we observe the data y(n) at discrete points as a function of θ, every $\pi/8$ radians, letting the positive vertical axis correspond to $\theta = 0(n = 0)$, and the counterclockwise direction as positive.

The observed values of y(n) are shown below in Table 1.

Table 1: Distorted Pattern Values

n	0	1	2	3	4	5	6	7	8	9	10-15
$y(n)$	0	3.061	5.657	8.922	10.828	11.087	9.657	6.757	2.828	1.531	0

In addition, suppose that the desired free space pattern is <u>known</u> to be:

$$\rho = -8 \sin \theta \qquad , \ 0 \le \theta \le \pi$$
$$= 0 \qquad\qquad , \text{ otherwise.}$$

as shown by the dotted circle in Figure 19. Its pattern values are:

Table 2: Free Space Pattern Values

n	0	1	2	3	4	5	6	7	8-15
$x(n)$	0	3.061	5.657	7.391	8	7.391	5.657	3.061	0

Using the data in Tables 1 and 2, the constants α and n_0 used in equation 20 will be evaluated.

$$y(n) = x(n) + \alpha x(n - n_0). \tag{20}$$

With α and n_0, the effects of the reflection can be eliminated in the measurements of <u>unknown</u> antenna patterns.

These quantities will now be evaluated. Because we deal with discrete data, the discrete Fourier transform will be used.[*] The cepstrum of $x(n)$ can be computed.

---

[*]Oppenheim and Schafer, <u>Digital Signal Processing</u>, Englewood Cliffs, N.J.: Prentice Hall, Ch. 3.

$$X(K) = \sum_{n=0}^{(N-1)} x(n)\varepsilon^{-j(2\pi/N)nK} \quad ; \quad n = 0,1,2,\ldots 15; \ N = 16.$$

$$\ln X(K) = \ln\left(\sum_{n=0}^{15} x(n)\varepsilon^{-j(\pi/8)nK}\right); \quad n = 0,1,2,3 \ldots 15$$

$$x'(n) = \sum_{K=0}^{15} \ln(X(K))\varepsilon^{+j(\pi/8)Kn}; \quad K = 0,1,2,\ldots, 15$$

$$\equiv \text{cepstrum of } x(n).$$

Next calculate the cepstrum of $y(n)$.

$$Y(K) = \sum_{n=0}^{(N-1)} y(n)\varepsilon^{-j(2\pi/N)nK}; \quad n = 0,1,2,3 \ldots 15; \ N = 16$$

$$= \sum_{n=0}^{15} [x(n) + \alpha x(n - n_0)]\varepsilon^{-j(\pi/8)nK}$$

$$= X(K)(1 + \alpha\varepsilon^{-j(2\pi/N)n_0 k})$$

$$\ln(Y(K)) = \ln(X(K)) + \ln(1 + \alpha\varepsilon^{-j(2\pi/N)n_0 k})$$

$$\simeq \ln(X(K)) + \alpha\varepsilon^{-j(2\pi/N)n_0 k}; \quad |\alpha| \ll 1.$$

$$y'(n) = \sum_{k=0}^{15} \ln(Y'(K)\varepsilon^{j(\pi/8)Kn}$$

$$= x'(n) + \alpha\delta(n - n_0)$$

Therefore

$$\alpha\delta(n - n_0) = y'(n) - x'(n) \tag{21}$$

In this particular case, calculations yield:

$$\alpha = 0.5, \tag{22a}$$

$$n_0 = 2. \tag{22b}$$

34

In other words, given an antenna whose free-space pattern $x(n)$ is known, measure its response $y(n)$ on the range where a reflection may exist. Using the calculations outlined above, determine the constants α and n_0. The results labeled (22a), (22b) indicate that they will appear as a data point or impulse of magnitude α at point n_0. If more than one reflection exists, additional impulses will appear in (21).

In practice, these calculations will be done on a computer, However, a sample calculation can be accomplished with a hand calculator.

The use of this technique is subject to the same limitation as fence installations and absorbing material. Changes in frequency range, etc. may introduce additional reflections and require a new determination of the α's and n_0's.

With these constants for a given antenna range, the true free-space pattern of an antenna can be calculated from its measured pattern and the use of (20), rearranged.

Again, assume that the pattern shown as the solid line in Figure 19 has been measured. Furthermore, assume that the range has been calibrated and that

$$\alpha = 0.5,$$
$$n_0 = 2.$$

These quantities can be determined by the geometric optical method or the cepstrum method as discussed above.

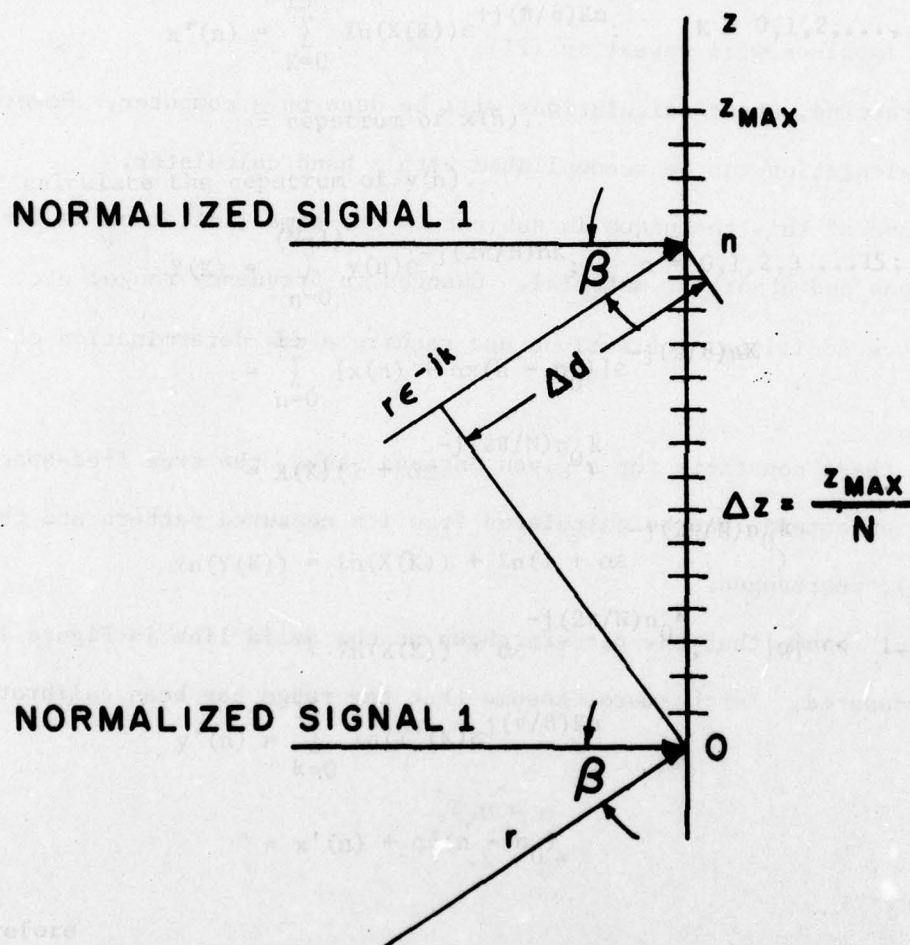With α and n_0 known, $x(n)$ can be determined from the above equation;

35

NORMALIZED SIGNAL 1

NORMALIZED SIGNAL 1

z

z_{MAX}

β

Δd

$r\epsilon^{-jk}$

n

$\Delta z = \dfrac{z_{MAX}}{N}$

O

β

r

Figure 20. Use of Probe Data and Fourier Transform
to Determine Reflected Data.

36

i.e.,

$$x(n) = y(n) - \alpha x(n - n_0)$$
$$= y(n) - 0.5x(n - 2).$$

Application of this equation yields the value of $x(n)$, the true pattern, shown in Table 3 in Figure 19. This pattern is shown as the dotted-line circle, $\rho = -2r \sin \theta = -8 \sin \theta$, in Figure 19. These are the same data as listed in Table 2, page 14.

2.6 Alternate Technique of Signal Processing

The example in the last section illustrates a method of resolving a scalar multipath signal into its direct and reflected components. This method may not be applicable to vector signals. However, some classes of vector signals can be analyzed in an analogous way.

The example below demonstrates a technique of determining the source (location and magnitude) of a disturbing reflection using the Fourier transform alone. Figure 20 describes the situation. The electric field is probed in the vertical (Z) direction and an approximately periodic pattern such as Figure 8 is recorded.

Assume that at the origin the received signal is a maximum, i.e., the direct and reflected signal are in phase giving

$$y(o) = 1 + r.$$

At any position n, the path length of the directly incident signal is approximately the same but the reflected signal has traveled an added distance:

37

$$\Delta d = \frac{Z_{max}}{N} (n)(\sin \beta).$$

The received signal of wavelength λ may be written as:

$$y(n) = 1 + r\varepsilon^{-j(Z_{max}/\lambda)(2\pi/N)(n)(\sin\beta)}$$

$$= 1 + r\varepsilon^{-jk_o(2\pi/N)n} ; \qquad k_o = \frac{Z_{max}}{\lambda} \sin \beta. \qquad (23)$$

Recall that the discrete Fourier transform is defined as:

$$Y(k) = \frac{1}{N} \sum_{n=0}^{(N-1)} y(n)\varepsilon^{-j(2\pi/N)kn}$$

$$= \frac{1}{N} \sum_{n=0}^{(N-1)} (1 + r\varepsilon^{-j(2\pi/N)(k_0)(n)})\varepsilon^{-j(2\pi/N)kn}$$

$$= \delta(k) + r\delta(k + k_0), \quad \delta(k)=1, \ k=0 \text{ and } \delta(k)=0 \text{ otherwise.} (24)$$

Examination of this result reveals that the Fourier transform of $y(n)$ consists of two impulses. The impulse at the origin is due to the direct signal and the delayed impulse results from the reflection. In this example the direct signal has been assumed to have an amplitude of one. The ratio of the magnitudes of the two impulses gives the relative value of the reflection. This quantity has been denoted by α in the previous problem.

The delay, k_o, allows determination of the direction (and, in turn, the location) of the reflection from the earlier formula

$$k_o = \frac{Z_{max}}{\lambda} \sin \beta$$

or

$$\sin \beta = \frac{k_o \lambda}{Z_{max}} .$$

In fact, when r and k_o have been determined, the true antenna pattern can be determined.

Suppose r and k_o are known, we may represent an arbitrary antenna pattern as:

$$y(n) = x(n)[1 + r\varepsilon^{-j(2\pi/N)k_o n}]$$

where x(n) is the pattern if no reflection were present.

The magnitude of the measurement may be represented as:

$$|y(n)| = \sqrt{x^2(n)\left[(1 + r\cos\frac{2\pi}{N}nk_o)^2 + r\sin\frac{2\pi}{N}nk_o)^2\right]}$$

All the quantities in this expression are known except x(n) which can be evaluated at every data point, n.

To illustrate this method it is applied to the data recorded in Fig. 8. Note that the units of this data are decibels (db). An arbitrary reference level was assumed and the data was converted to the units of voltage. Following this, the Fast-Fourier Transform was taken. The result is shown in the table below.

Examining Y(k) in Table 4 shows that there is reflection corresponding to $k_o = k = 5$. The value of the impulse at k=5 is 1.46. However, the value of the impulse at k=0 in Table 4 due to the direct signal is 8.92.

Therefore, the relative magnitude of the reflection, r_1, is the ratio of these two numbers. This is a specific value for the quantity r shown, in equation (23) and (24).

Its relative magnitude is:

$$r_1 = \frac{1.46}{8.92} = 0.16$$

Its direction is determined by the formula:

39

Table 4. Electric Field Probe Data and Its FFT
(from Figure 8)

n	y(n)	$\lvert Y(k) \rvert = \lvert \frac{1}{N} \sum\limits_{n=0}^{(N-1)} y(n)\epsilon^{-j(2\pi/N)kn} \rvert$	k
0	5.82	8.92	0
1	8.91	0.32	1
2	12.02	0.17	2
3	9.33	0.17	3
4	6.10	0.82	4
5	11.89	1.46	5
6	11.89	0.23	6
7	3.98	0.31	7
8	10.0	0.11	8
9	13.03	0.31	9
10	7.08	0.23	10
11	7.08	1.46	11
12	10.0	0.82	12
13	7.94	0.17	13
14	7.59	0.17	14
15	10.12	0.32	15

$$k_o = \frac{Z_{max}}{\lambda} \sin \beta$$

$$\sin \beta = \frac{\lambda k_o}{Z_{max}} = \frac{1}{16}(5); \quad \lambda = 1'; \quad Z_{max} = 16'.$$

$$\beta = 18.2°$$

Using the optical method described earlier in the report, it was determined that the major reflections came from a direction bracketed by

angles of 16.7° to 18.1 degrees.

Further examination of Table 4 indicates that there is a reflection corresponding to $k = 4$. Its magnitude is $r_2 = 0.09$. The recorded data in Figure 8 indicate that there is more than one reflection. In order to interpret the remaining points in $Y(k)$, further study is required. However, the technique does show enough promise to warrant that study.

2.7 Conclusion

Elimination of the effects of reflecting signals is necessary on outdoor antenna ranges if meaningful pattern data is to be obtained.

The proper use of reflecting fences can be very effective in eliminating reflections. However, a particular installation may be useful for only a limited frequency range. This is because usually the beam width or aperture of the illuminating antenna varies with frequency, and thus exposes more (or less) of the surroundings to radiation, giving rise to additional reflections.

Providing fences to be effective for the general case would require an effort which may be practically prohibitive. If the beam width or pattern of the illuminating antenna changes (say, because of mechanical misalignment of its elements or changes in frequency of the input signal), additional reflections will probably be introduced. Therefore, it is important to invest in illuminating antennas which meet the specifications for which the constructed fences were designed and insure that they are installed properly.

In addition, absorbing material also can eliminate reflections. It is most useful in eliminating reflections from portions of the receiving structure. It is too expensive to replace fences eliminating ground reflections and offers no particular advantages.

41

Finally, the elimination of the effects of reflections by processing the observed data would represent a large saving in time and effort. Most of the equipment to implement this technique is already in place. Data processing equipment is already used to process the measurements. Also, the range equipment is calibrated every day before measurements begin, using standard gain horns. These could be used for cepstrum determination.

Furthermore, the particular method outlined here is only one of several based on this general technique. For instance, the antenna could be fixed in place and a known signal as a function of time recorded at the receiver. This time dependent data could be processed rather than the spatial data to yield the same information. Practical considerations would decide which specific method to implement. The application of cepstrum analysis to this problem as described in this report shows promise and should be pursued.

3. INCREASED FREQUENCY COVERAGE: 18 GHz – 40 GHz

3.1 Introduction

The IEEE, in its recent Standard Letter Designations for Radar Frequency Bands, has designated 18-27 GHz as K band and 27-40 GHz as Ka band. Note that these frequencies correspond to free-space wavelengths of 1.67 cm to 0.75 cm. One-quarter wavelength of a 40 GHz signal is less than 2mm in length. Vibrations or mechanical variations of an aircraft structure of this order of magnitude can have profound effects on the performance of antenna mounted on the aircraft unless they are designed to be immune to these effects.

Also, there are well-known oxygen and water absorption lines above 20 GHz. This causes atmospheric transmission characteristics to vary with weather. These data should be obtained before beginning antenna tests in this frequency range. See Figure 21.

3.2 Equipment: Receivers

The Scientific-Atlanta, Inc. series 1711 Microwave Measurement Receiver covers the frequency range of 2.0 GHz to 40.0 GHz. The receiver has a dynamic range of 60 db and a sensitivity of (-75) dbm in the 20-40 GHz frequency range. A series of RF to IF waveguide mixers is used to cover this range. Model (13A-18) Tunable Waveguide mixer covers 18-26.5 GHz and model (13A-26) covers 26.5-49.0GHz.

In fact, the frequency range of the receivers in use at the Newport sites can be extended to 40 GHz by the addition of these waveguide mixers.

43

3.3 Equipment: Signal Sources

Several manufacturers market signal generators in this frequency range with power outputs up to the order of 100 mw. Higher power sources do not seem to be available (1977).

However, traveling-wave tube amplifiers are available with power outputs of over 1 kW (e.g. from Hughes Aircraft Company). There are a number of radar systems operating in this frequency range and there are many device, component, and system manufacturers active in the millimeter wave area.[†]

Listed below are the specifications of two instruments currently available.

Manufacturer	Model Number	Frequency Range	Power Output
Watkins-Johnson Co.	WJ-1250	18–26.5 GHz	10 mW
		26.5–40 GHz	5 mW
Hewlett Packard Co.	938A	18–26.5 GHz	Output depends on
	940A	26.5–40 GHz	input. 0.5–1.0 mW (typical)

> Note: The H-P 938A and 940A are frequency doublers and require input drivers.

The required power output of the signal source can be estimated as follows.

$$P = S + N - G_R + T_L^* - G_T$$

where P = Required power output of signal source in dbm.

           S = Sensitivity of receiver in dbm.

           N = Variations of maxima to nulls in pattern in db.

[†] See *Microwave Journal*, Vol. 20, No. 11, November 1977

[*] See *Reference Data for Radio Engineers*, 4th edition, ITT Corp. Fig. 32, page 752. Fig. 21 of this report indicates that loss due to water vapor and oxygen absorption will be less than 1 db.

G_R = Receiver antenna gain in db.

T_L = Transmission attenuation in db.

G_T = Transmitter antenna gain in db.

Some estimates of required power are listed in the table below.

The smallest estimate is obtained if a frequency of 20 GHz is considered and the Short Range (distance about 0.25 km.) is used. In all calculations, S = -75 dbm and G_R = 0 db. In this particular case T_L = 109 db; let N = 30 db and G_T = 30 db. Then:

$$P = S + N - G_R + T_L - G_T \quad ; \text{(Short Range, 20 GHz)}$$

$$= -75 + 30 + 0 + 109 - 30$$

$$= 34 \text{ dbm}$$

$$= 2.5 \text{ watts}$$

The largest power estimate is obtained if 40 GHz signal sources on Range #2 (distance about 2.5 km) with N = 40 db and G_T = 30 db are considered.

Then: $\quad P = S + N - G_R + T_L - G_T \quad ; \text{(Range #2, 40 GHz)}$

$$= -75 + 40 + 0 + 132 - 30$$

$$= 67 \approx 70 \text{ dbm}$$

$$= (10)^4 \text{ watts}$$

The gain of the transmitting antenna is a parameter under the designer's control and, obviously, is very important. Here G_T is assumed to be 30 db. Any change in its value directly affects the required power of the signal source.

The published sensitivity specification in the 26 to 40 GHz range for the Scientific-Atlanta, Inc. receiver, series 1740, which employs phase-lock techniques, is -100 dbm. Of course, using this receiver sensitivity in the above calculations reduces the required signal power by 25 db. However, in addition, a phase-lock reference input that is 35 db greater than the signal channel is needed.

45

Table 5   Required Signal Power

Range	Freq.	S	N	G_R	T_L	G_T	P(dbm)	P(watts)
Short	20	75	30	0	109	30	34	2.5
Short	40	75	40	0	115	30	50	100
#2	20	75	30	0	126	30	50	100
#2	40	75	40	0	132	30	90	$(10)^4$

3.4 Conclusions

The short wave lengths corresponding to this frequency range require increased attention to mechanical details in making measurements.

The absorption by oxygen and water of electromagnetic energy in this frequency range causes increased atmospheric transmission loss.

Receiving equipment in this frequency range is available. Transmitting equipment may not be available off the shelf, but it can be provided on special order.
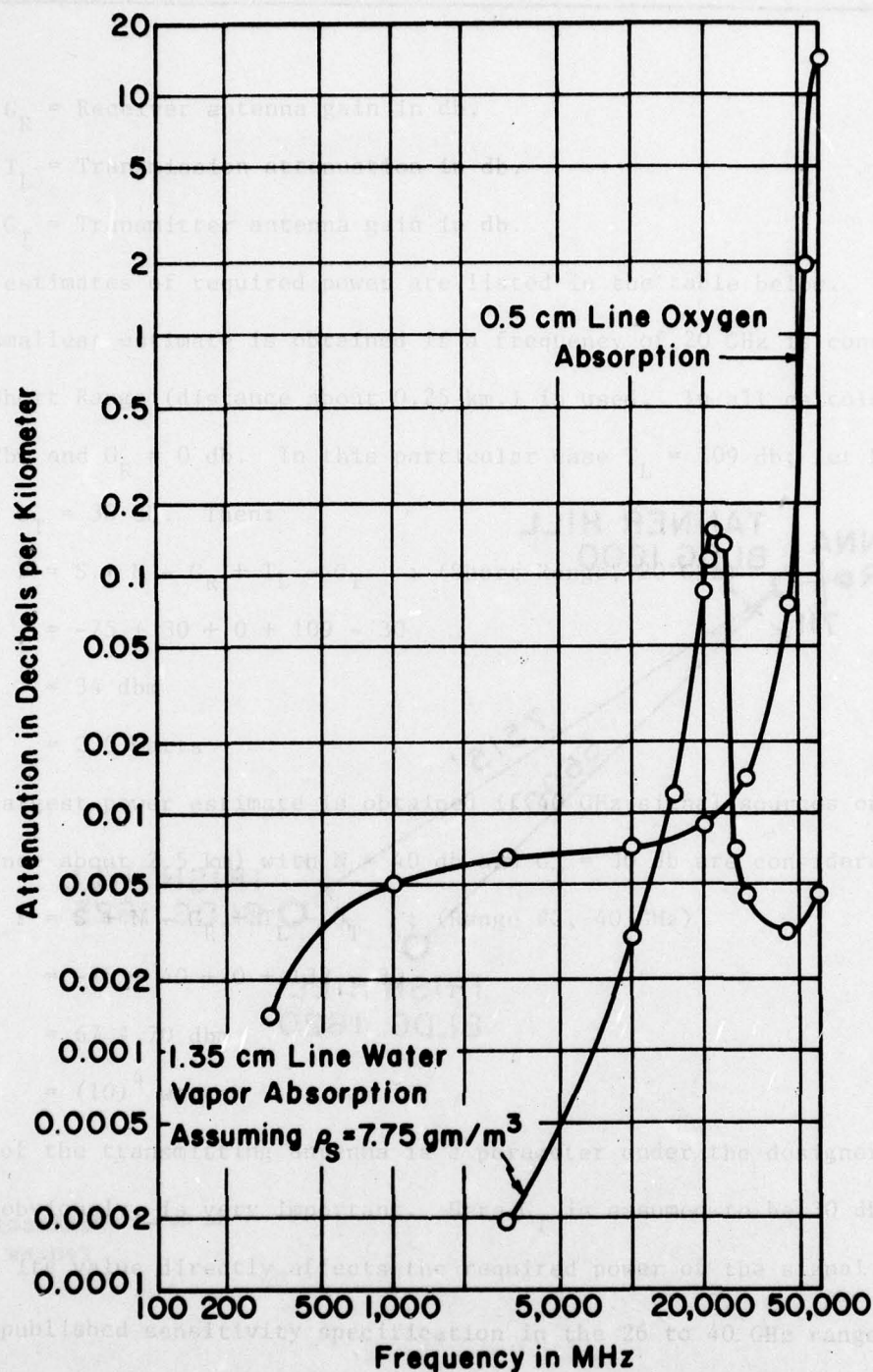
46

Figure 21. Atmospheric Absorption by the 1.35 cm Line of Water Vapor and the 0.5 cm Line of Oxygen. Water Vapor Absorption Calculated for the Mean Absolute Humidity at Washington, D.C. (From NBS Report 6763, Attenuation of Microwaves, by B.R. Bean and L.P. Riggs, April 21, 1961)
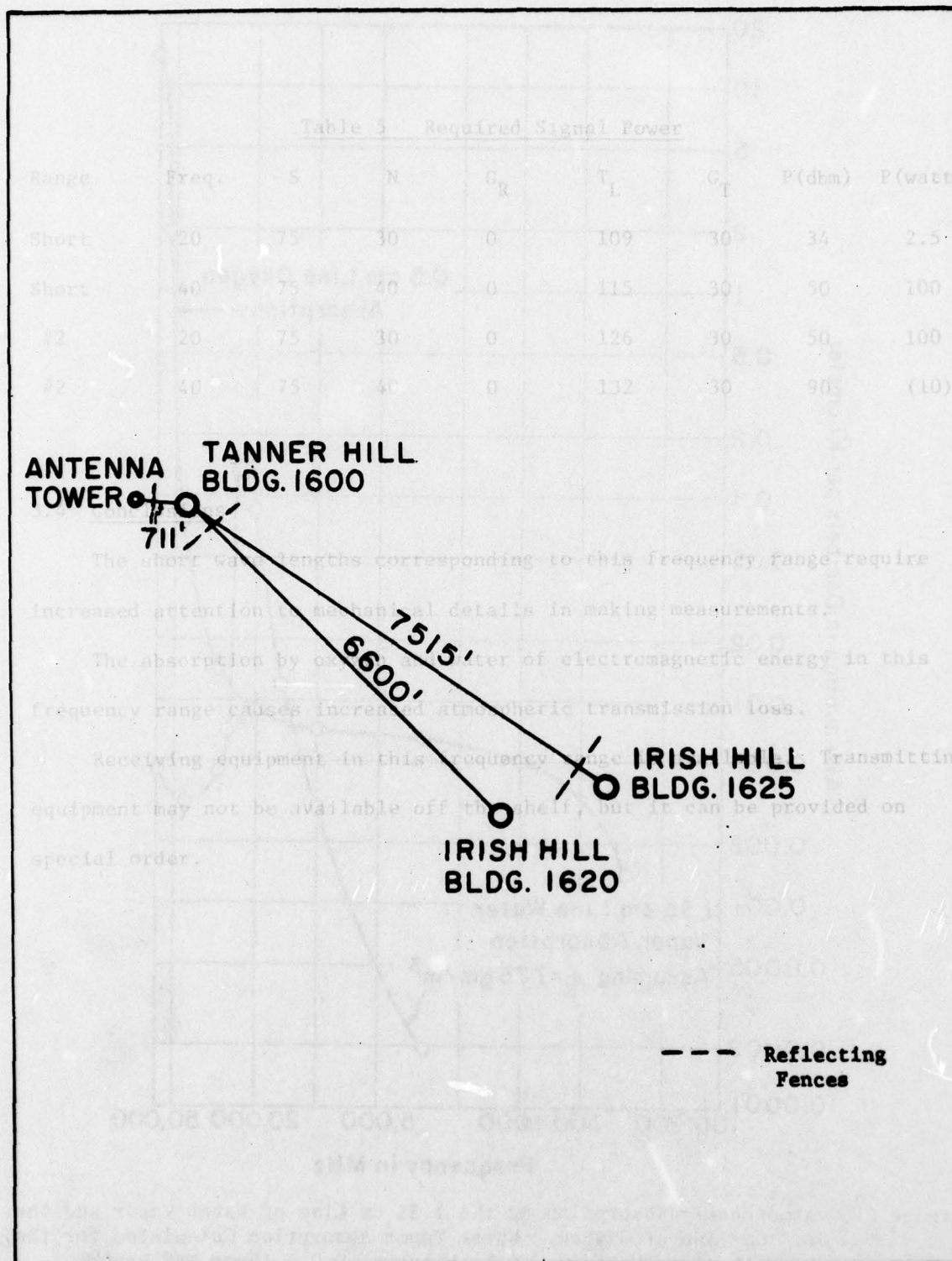
ANTENNA
TOWER

TANNER HILL
BLDG. 1600

711'

7515'

6600'

IRISH HILL
BLDG. 1625

IRISH HILL
BLDG. 1620

N

- - - Reflecting
Fences

Figure 22. Approximate Location of Reflecting Fences
Installed at RADC Antenna Test Site.

48

Appendix 1

REPORTS OF EARLIER RADC STUDIES

1. "Investigation of Precision Antenna Pattern Recording and Display Techniques," Final Report, AD415-912, March, 1963.

2. "Investigation of Precision Antenna Pattern Recording and Display Techniques, Phase II, Final Report, J. Searcy Hollis et al, AD630-124, February 1966.

3. "Error Analysis for the RADC F-4 Antenna Test Facility, Final Report, Mario Macera, RADC-TR-74-309, December 1974, B001090L.
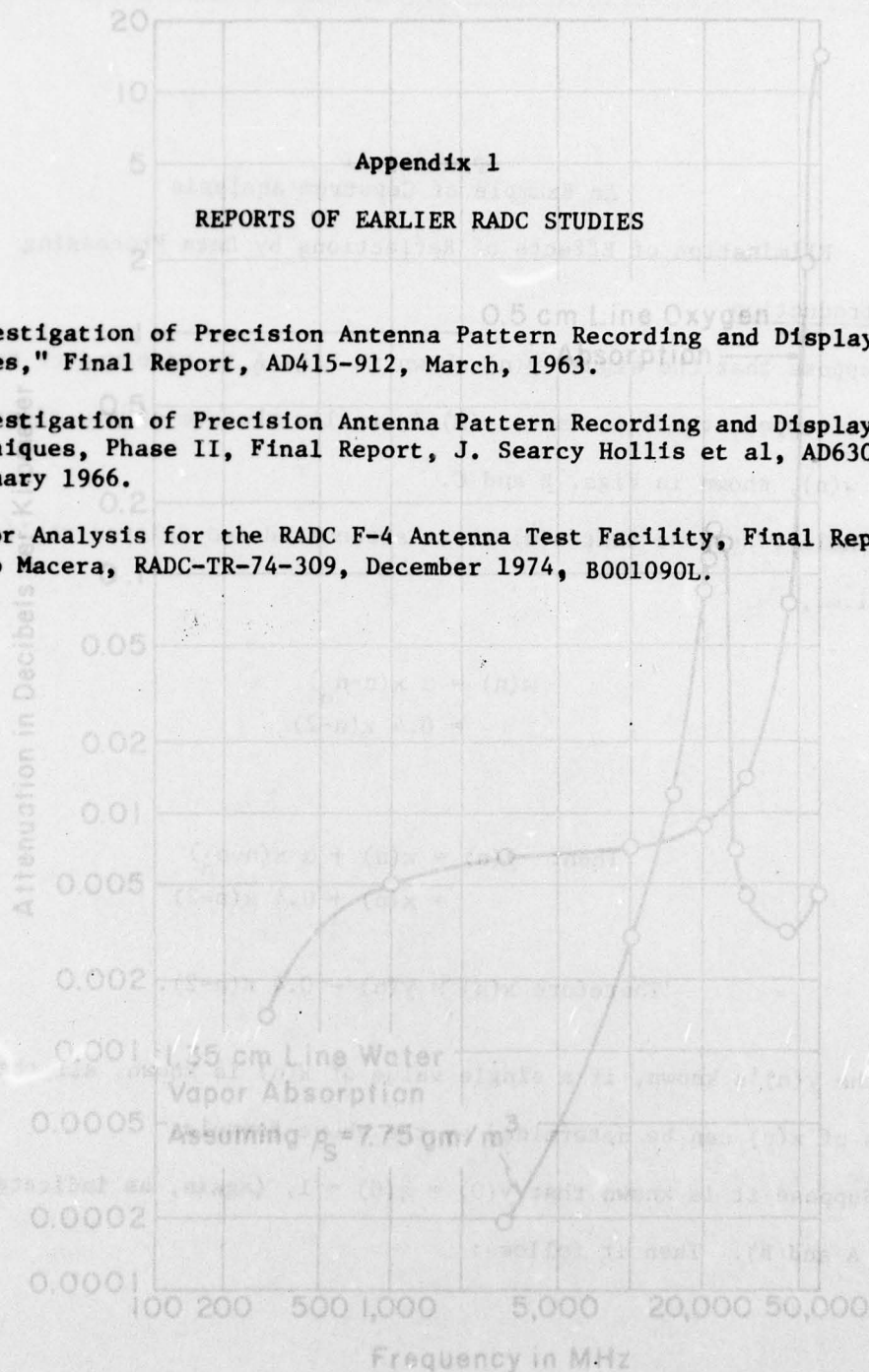
Figure 21. Atmospheric Absorption by the 1.35 cm Line of Water Vapor and the 0.5 cm Line of Oxygen. Water Vapor Absorption Calculated for the Mean Absolute Humidity at Washington, D.C. (From NBS Report 6763, Attenuation of Microwaves, by B.R. Bean and L.P. Riggs, April 21, 1961)

Appendix II
An Example of Cepstrum Analysis

Elimination of Effects of Reflections by Data Processing

I. Introduction

Suppose that the signal $y(n)$ shown in Fig. A is received or measured.

Further, suppose that, in fact, $y(n)$ is really the sum of two signals,

$x(n) + w(n)$, shown in Figs. B and C.

Finally, suppose that $w(n)$ is an attenuated and delayed replica of

$x(n)$; i.e.,

$$w(n) = \alpha\, x(n-n_o)$$
$$= 0.4\, x(n-2)$$

Then: $y(n) = x(n) + \alpha\, x(n-n_o)$
$$= x(n) + 0.4\, x(n-2)$$

Therefore $x(n) = y(n) - 0.4\, x(n-2)$.

With the $y(n)$'s known, if a single value of $x(n)$ is known, all the other

values of $x(n)$ can be determined by the above formula.

Suppose it is known that $y(0) = x(0) = 1$, (again, as indicated in
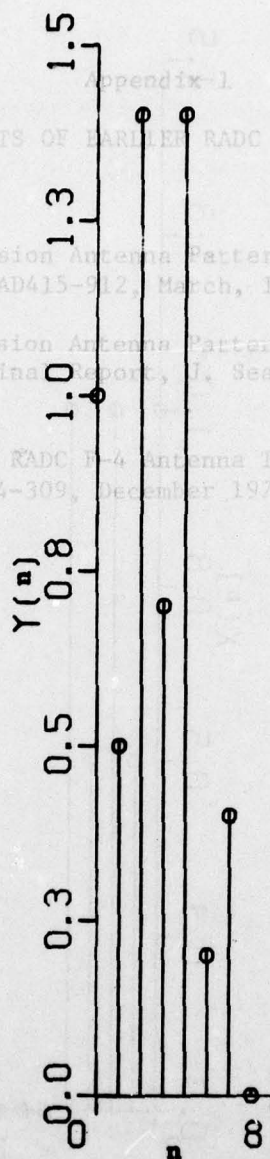
Figs. A and B). Then it follows:

Fig. A. $y(n) = x(n) + \alpha\, x(n-n_o)$

-Y(N)

An Example of Cepstrum Analysis

Elimination of Effects of Reflections by Data Processing

I. Introduction

Suppose that the signal y(n) shown in Fig. A is received or measured. Further, suppose that, in fact, y(n) is really the sum of two signals, x(n) + w(n), shown in Figs. B and C.

Finally, suppose that w(n) is an attenuated and delayed replica of x(n); i.e.,

$$w(n) = \alpha\, x(n-n_0)$$
$$= 0.4\, x(n-2)$$

Then: $y(n) = x(n) + \alpha\, x(n-n_0)$
$$= x(n) + 0.4\, x(n-2)$$

Therefore $x(n) = y(n) - 0.4\, x(n-2)$.

With the y(n)'s known, if a single value of x(n) is known, all the other values of x(n) can be determined by the above formula.

Suppose it is known that $y(0) = x(0) = 1$, (again, as indicated in Figs. A and B). Then it follows:
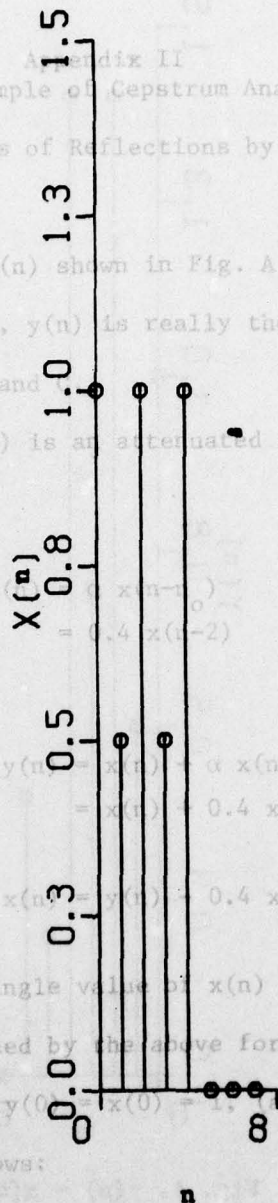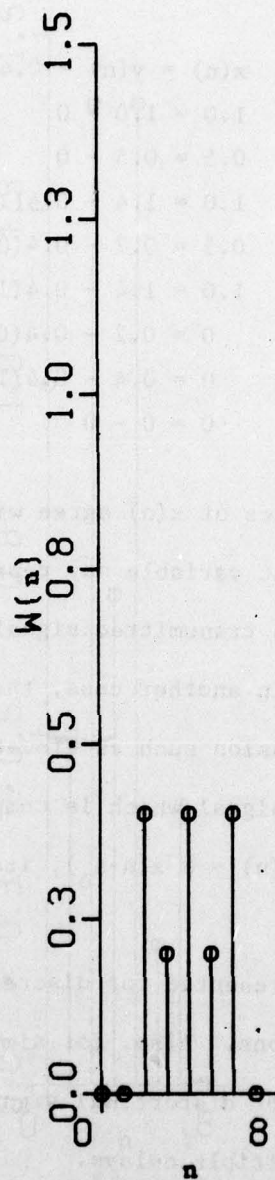$$y(n) = x(n) + \alpha\, x(n-n_0)$$

Fig. B. x(n)

X(N)

52

$W(n)$

n

Fig. C. $w(n) = \alpha\, x(n-n_o)$

$W(N)=A*X(N-N\emptyset)$

n	y(n)	x(n) = y(n) - 0.4 x(n-2)
0	1.0	1.0 = 1.0 - 0
1	0.5	0.5 = 0.5 - 0
2	1.4	1.0 = 1.4 - 0.4(1.0)
3	0.7	0.5 = 0.7 - 0.4(0.5)
4	1.4	1.0 = 1.4 - 0.4(1.0)
5	0.2	0 = 0.2 - 0.4(0.5)
6	0.4	0 = 0.4 - 0.4(1.0)
n > 6	0	0 = 0 - 0

Of course, these values of $x(n)$ agree with those of Fig. B.

Note: The independent variable may represent time. Then the received signal $y(n)$ results when a transmitted signal $x(n)$ is distorted by a multipath transmission link. In another case, the independent variable may represent a physical dimension such as elevation or azimuth. Then $y(n)$ may represent a received signal which is composed of a directly transmitted signal $x(n)$ plus $w(n) = \alpha\, x(n-n_o)$, its reflection from some local obstacle.

The development is presented for discrete data but applies equally as well to continuous functions. Also, for simplicity the discussion considers only one delayed (or distorting) signal; however, the analysis may be extended to include multiple delays.

2. Determination of α and n_o by Cepstrum Analysis

The above example was fabricated and since α and n_o were assumed, $x(n)$ was easily recovered when $y(n)$ was given.

A natural question to ask is the following: Can a given transmission link or antenna range be "calibrated"? Can α and n_o be determined so that any __unknown__ $x(n)$ can be recovered when $y(n)$ is received?

Fortunately, the answer to this question is yes. If a __known__ signal, $x(n)$, is transmitted and the received signal, $y(n)$, is recorded, the technique of cepstrum[*] analysis will yield α and n_o.

Again, consider the equation:

$$y(n) = x(n) + \alpha\, x(n-n_o)$$

In this case, __the $y(n)$'s and $x(n)$'s are known.__ The constants α and n_o are to be determined. This can be done as follows:

First, take the Discrete Fourier Transform

$$Y(k) = \sum_{n=0}^{(N-1)} y(n)\, \epsilon^{-j \frac{2\pi}{N} n k}$$

$$= \sum_{n=0}^{(N-1)} x(n)\, \epsilon^{-j \frac{2\pi}{N} n k} + \alpha \sum_{n=0}^{(N-1)} x(n-n_o)\, \epsilon^{-j \frac{2\pi}{N} n k}$$

$$= X(k)\, (1 + \alpha\, \epsilon^{-j \frac{2\pi}{N} n_o})$$

where $Y(k)$ is the Discrete Fourier Transform of the function $y(n)$ and $X(k)$

---

[*] Bogert, Healy, Tukey, "The Quefrency Analysis of Time Series for Echoes", Proc. Symposium on Time Series Analysis, M. Rosenblatt (ed.), J. Wiley, 1963.

is the Discrete Fourier Transform of x(n). N represents the total number of
points of data.

Next, take the logarithm of each side:

$$\ln(Y(k)) = \ln(X(k)) + \ln(1 + \alpha \, \epsilon^{-j \frac{2\pi}{N} n_o k})$$

$$= \ln(X(k)) + \alpha \, \epsilon^{-j \frac{2\pi}{N} n_o k}; \; \alpha \ll 1$$

Note: The assumption, $\alpha \ll 1$, is made to simplify and clarify the
analysis. If α is not small, this development still applies.

Finally, take the inverse Discrete Fourier Transform

$$y'(n) = \sum_{k=0}^{(N-1)} \ln(Y(k)) \, \epsilon^{j \frac{2\pi}{N} k n}$$

$$= \sum_{k=0}^{(N-1)} [\ln(X(k)) + \alpha \, \epsilon^{-j \frac{2\pi}{N} k n_o}] \, \epsilon^{j \frac{2\pi}{N} k n}$$

$$= x'(n) + \alpha \, \delta \, (n - n_o)$$

$$\alpha \, \delta(n - n_o) = y'(n) - x'(n).$$

The left-hand side of the equation is the desired result. It is an
impulse of strength α located at position n_o. Because y(n) and x(n) are
known, y'(n) and x'(n) can be calculated, and α and n_o have been deter-
mined.

After α and n_o have been determined for a particular experiment,
we may go back to the technique illustrated at the beginning of this

56

discussion and extract an <u>unknown</u> transmitted signal, $x(n)$, from the received signal $y(n)$; i.e.,

$$x(n) = y(n) - \alpha\, x(n-n_o).$$

3. Discussion

By examining the steps in the Cepstrum Analysis, insight is gained into why it works.

We begin with:

$$y(n) = x(n) + \alpha\, x(n-n_o)$$

The right-hand side of this equation may also be written as the convolution of the signal $x(n)$ and the characteristic function of the transmission link; i.e.,

$$y(n) = x(n) * h(n)$$

When the Fourier Transform is taken, the right-hand becomes a product; i.e.,

$$F(y(n)) = Y(K) = X(K)\, H(K)$$

The Fourier Transform is taken because of the form of $H(K)$. Recall if the Fourier Transform of $x(n)$ is $X(K)$, the Fourier Transform of $x(n-n_o) = X(K)\, \epsilon^{-j \frac{2\pi}{N} n_o}$. Now the inverse Fourier Transform of $\epsilon^{-j \frac{2\pi}{N} n_o}$ is an impulse at n_o which can be identified and will be useful.
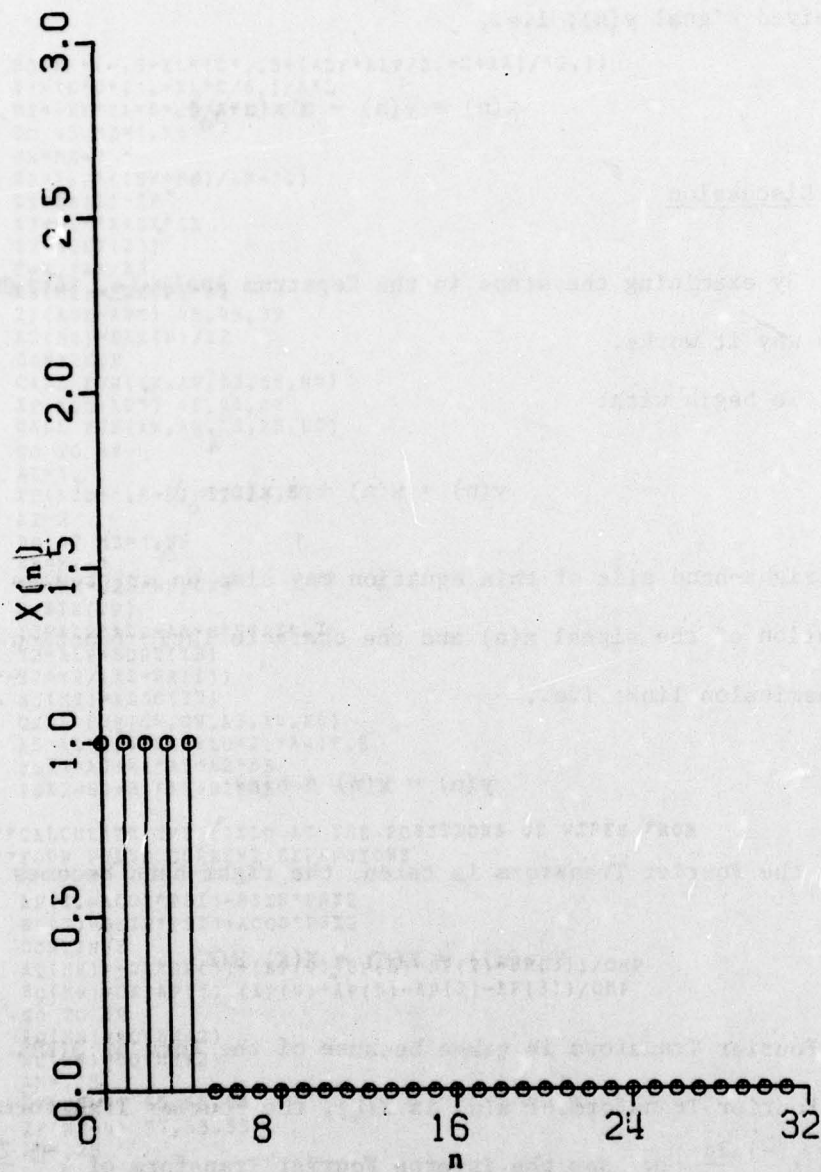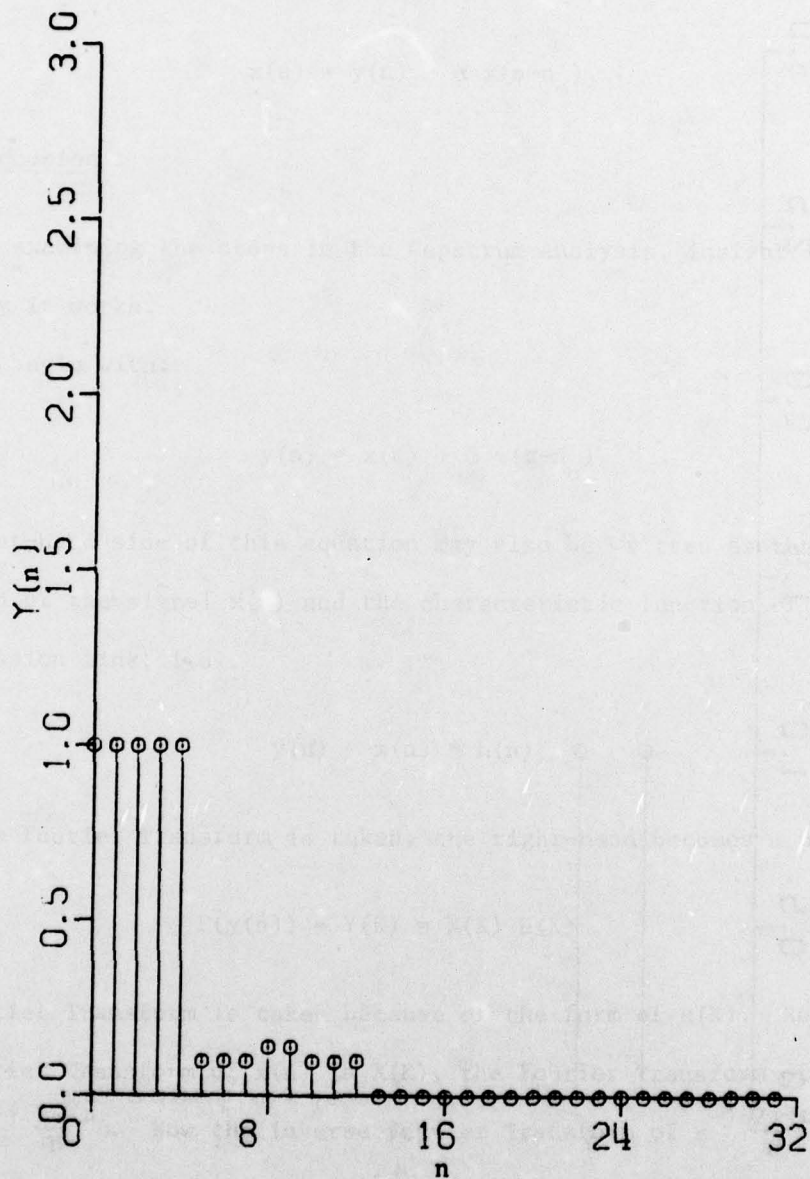
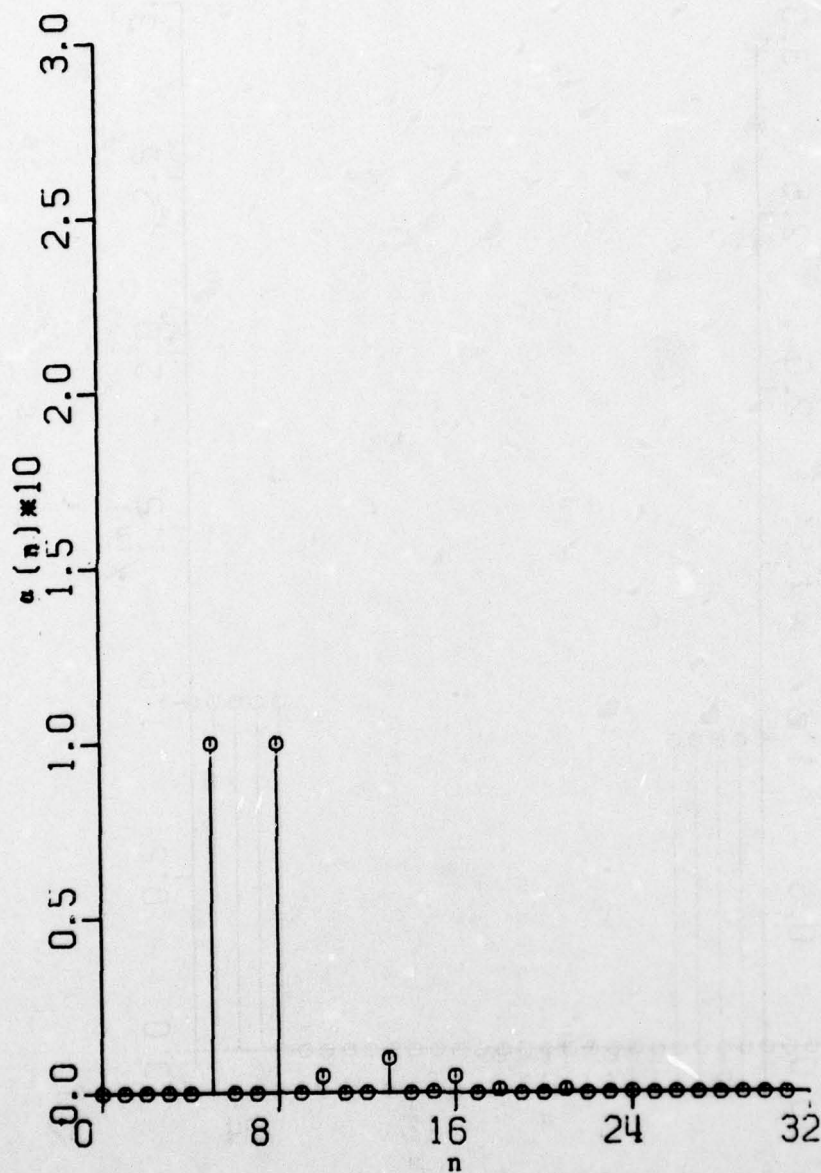Fig. D.   x(n) vs. n.

Fig. E. y(n) vs. n.

Figure F. $\alpha_0 \delta(n-n_0) + \alpha_1 \delta(n-n_1)$ vs. n.

60

However, this quantity is submerged in the product $X(K) H(K)$. But the $\ln XH = \ln X + \ln H$ and the product is transformed into a sum; i.e.

$$\ln (Y(K)) = \ln (X(K)) + \ln (H(K)))$$

Taking the inverse transform and rearranging it, the useful result emerges as

$$F^{-1} \ln(Y(k)) = y'(n) = x'(n) + \alpha \, \delta(n-n_o)$$

$$\alpha \, \delta(n-n_o) = y'(n) - x'(n)$$

This technique is illustrated in the example which follows. Consider a received signal:

$$y(n) = \left| x(n) + \alpha_o \, x(n-n_o) + \alpha_1 \, x(n-n_1) \right| ; \text{ where } |x| \text{ is the}$$
$$\text{magnitude of } x.$$
$$= \left| x(n) + 0.1 \, x(n-5) + j(0.1) \, x(n-8) \right|$$

Further, it is known that:

$$x(n) = 1 \quad , \quad n=0,1,2,3,4$$
$$= 0 \quad \text{otherwise}$$

To be more general, two reflections or delays are included, one of which has imaginary values. The data $y(n)$ and $x(n)$ are shown in Fig. D and E.

When this data is processed to ascertain the α_1's and the n_1's, the results are as shown in Fig. F. Note the $\alpha_0 = 0.1$ at $n_0 = 5$ and $\alpha_1 = 0.1$

61

at $n_1 = 8$.

Also, note the unwanted values at points: $2n_0 = 10$, $n_0 + n_1 = 13$, $2n_1 = 16$. These additional points result from the fact that:

$$\ln(1+\alpha) = \alpha - \frac{1}{2}\alpha^2 + \frac{1}{3}\alpha^3 + \text{---} + (-1)^{(1+n)}\frac{\alpha^n}{n} + \text{--}; \quad -1 < \alpha < 1; \quad n = 1,2,3\text{--}$$

In the discussion, the approximation was made that $\ln(1+\alpha) \approx \alpha$; $\alpha \ll 1$.

Because these spurious responses occur at multiples of n_0, n_1 and $(p\,n_0 + q\,n_1)$, where p and q are integers, they can be identified and ignored.

MISSION
of
Rome Air Development Center

RADC plans and conducts research, exploratory and advanced development programs in command, control, and communications (C^3) activities, and in the C^3 areas of information sciences and intelligence. The principal technical mission areas are communications, electromagnetic guidance and control, surveillance of ground and aerospace objects, intelligence data collection and handling, information system technology, ionospheric propagation, solid state sciences, microwave physics and electronic reliability, maintainability and compatibility.